OPTIMIZATION OF EXPRESSION AND ISOLATION OF A THERMOPHILIC P450 ENZYME

Yaprak ASLANTAŞ

İzmir Institute of Technology
December, 2018

OPTIMIZATION OF EXPRESSION AND ISOLATION OF A THERMOPHILIC P450 ENZYME

A Thesis Submitted to
the Graduate School of Engineering and Sciences of
İzmir Institute of Technology
in Partial Fulfillment of the Requirements for the Degree of

MASTER OF SCIENCE

in Biotechnology

by
Yaprak ASLANTAŞ

December 2018
İZMİR

We approve the thesis of **Yaprak ASLANTAŞ**

Examining Committee Members:

Asst. Prof. Nur Başak SÜRMELİ
Department of Bioengineering, İzmir Institute of Technology

Asst. Prof. Hatice Eser ÖKTEN
Department of Environmental Engineering, İzmir Institute of Technology

Asst. Prof. Hümeyra TAŞKENT SEZGİN
Departments of Genetics and Bioengineering, İzmir Economy University

3 December 2018

Asst. Prof. Nur Başak SÜRMELİ
Advisor, Department of Bioengineering
İzmir Institute of Technology

Assoc. Prof. Gülşah ŞANLI MOHAMED
Co-Supervisor, Department of Chemistry
İzmir Institute of Technology

Assoc. Prof. Engin ÖZÇİVİCİ
Head of the Programme of Biotechnology and Bioengineering

Prof. Aysun SOFUOĞLU
Dean of the Graduate School of Engineering and Applied Sciences

ACKNOWLEDGMENTS

I would first like to thank my thesis advisor Asst. Prof. Nur Başak SÜRMELİ. She always helped me and shared valuable information with me throughout my graduate studies.

This project was supported by The Scientific and Technological Research Council of Turkey (TUBITAK) 116Z380 grant. Also, I thank to İzmir Institute of Technology, Biotechnology and Bioengineering Applications and Research Centre (BIYOMER) for their instrumental help.

Besides, I thank to Asst. Prof Çağlar KARAKAYA and Asst. Prof Ali Oğuz BÜYÜKKİLECİ to allow usage of their devices.

These acknowledgements would not be complete without mentioning my laboratory friends who are Joana AGGREY-FYNN, Emre HAKLI, Ekin KESTEVUR, Gülce GÜRALP, Semih BAŞLAR and Fatmanur BOSTAN.

I also thank to Nüket POLAT, Fikrican DİLEK and Aykut ZELÇAK for experimental help and I am really thankful to encourage me my all friends during my thesis study.

I am so lucky and cheerful thanks to Osman KARABALCI who supports me from the heart even in my hardest moments. I heartfelt thank you to always with me.

Lastly, I must express the deepest gratitude to my family for providing me with unfailing support and continuous encouragement throughout my years of study and through the process of researching and writing this thesis. I am very grateful to them.

ABSTRACT

OPTIMIZATION OF EXPRESSION AND ISOLATION OF A THERMOPHILIC P450 ENZYME

Cytochrome P450 enzymes (CYP or P450) are monooxygenases that catalyze the oxidation of hydrocarbons with high efficiency and selectivity, and many other reactions like hydroxylation, epoxidation, reduction, demethylation. CYP119, is a thermophilic P450 from *Sulfolobus acidocaldarius*. Thanks to thermophilic properties, CYP119 has potential to be widely used as a biocatalyst in production of fine chemicals and pharmaceuticals. However, production and purification of CYP119s is quite difficult and time consuming. Here, through recombinant protein production techniques, the optimum production and purification of heat-tolerant CYP119 has been successfully carried out. N-terminal and C-terminal histidine tags were cloned to CYP119. Protein expression was induced in *Escherichia coli BL21 (DE3*) cells with isopropyl β-D-1-thiogalactopyranoside (IPTG). δ-aminolevulinic acid (ALA) was also used to increase the heme biosynthesis. Different IPTG and ALA concentrations, expression temperature and duration were used to optimize production. CYP119 was isolated and purified with Ni-NTA affinity column. The thermostability of purified N (N-His-CYP119) and C (C-His-CYP119) terminal His-tagged were compared with wild type CYP119 (Wt-CYP119). Oxidation reaction of CYP119 and variants carried out and compared at 25 °C and 65 °C. Also, epoxidation of styrene was performed with N-His-CYP119 in different temperatures. The effects of histidine tags on stability and activity of the CYP119s were observed. Here, conditions for the production of CYP119 were optimized and the histidine tags were found to cause changes in stability and function of proteins. This project will lead to increase in the production of the important enzyme CYP119, which will increase its utilization in the industry.

ÖZET

BİR TERMOFİLİK P450 ENZİMİNİN EKSPRESYONUNUN VE İZOLASYONUNUN OPTİMİZASYONU

Sitokrom P450 enzimleri (CYP veya P450) hidrokarbonların oksidasyonunu yüksek verimlilik ve seçicilikle katalizleyen ayrıca hidroksilasyon, epoksidasyon, redüksiyon, demetilasyon gibi pek çok reaksiyonu olan monooksijenez enzimleridir. CYP119, *Sulfolobus acidocaldarius* arkesinden elde edilen asidotermofilik bir P450 enzimidir. CYP119 termofilik özelliği sayesinde ince kimyasalların ve farmasötiklerin üretiminde bir biyokatalizör olarak yaygın bir şekilde kullanılma potansiyeline sahiptir. Ancak tüm bu özelliklerinin yanında CYP119'un üretimi ve saflaştırılması oldukça zor ve zaman alıcıdır. Bu çalışmada, recombinant protein üretimi teknikleri sayesinde termofilik CYP119'un optimum üretimi ve saflaştırılması başarıyla gerçekleştirildi. CYP119 DNA'sına N-terminal ve C-terminal histidin etiketleri klonlandı. Protein ekspresyonu izopropil β-D-l-tiyogalaktopiranosid (İPTG) ile *Escherichia coli BL21 (DE3)* hücrelerinde indüklendi. Ayrıca hem biyosentezini artırmak için δ-aminolevülinik asit (ALA) kullanıldı. Üretimi optimize etmek için farklı IPTG ve ALA konsantrasyonları, ekspresyon sıcaklıkları ve süreleri kullanıldı. CYP119, Ni-NTA afinite kolon ile izole edildi ve saflaştırıldı. Saflaştırılan N (N-His-CYP119) ve C (C-His-CYP119) terminal Histidin etiketli CYP119'ların termostabiliteleri doğal yapıdaki CYP119'un (d-CYP119) termostabilitesi ile karşılaştırıldı. CYP119 ve varyantlarının oksidasyon tepkimeleri 25 °C ve 65 °C'de gerçekleştirildi ve karşılaştırıldı. Ayrıca N-His-CYP119'un epoksidasyonu HPLC ile farklı sıcaklıklarda izlendi. Tüm bunların yanı sıra izolasyonu kolaylaştırmak için CYP119' un hem N terminaline hem de C terminaline klonlanan Histidin etiketlerinin termostabiliteye ve aktiviteye olan etkileri araştırıldı. Çalışmanın sonunda CYP119 üretimi için koşullar optimize edildi ve Histidine etiketinin proteinlerin kararlılığında ve fonksiyonlarında değişikliklere yol açtığı bulundu. Bu çalışma sayesinde CYP119 gibi oldukça önemli enzimlerin ilaç ve kimya sanayinde kullanımlarında artış sağlanacak ve protein izolasyonunda sıklıkla kullanılan Histidin etiketleri daha dikkatli kullanılacaktır.

TABLE OF CONTENTS

LIST OF FIGURES

Figure **Page**

LIST OF TABLES

Table **Page**

CHAPTER 1

INTRODUCTION

1.1. Overview of Biocatalysts

Biocatalysts are enzyme systems that catalyze reactions in biological systems. Biocatalysis is a strong tool for selective oxidations and it has more applications in addition to the classical chemical synthesis of fine chemicals and pharmaceuticals[1]. Thanks to the advances in bioengineering and enzyme technology techniques, there is a considerable progress in the development of biocatalysts. Biocatalysts have diverse applications in many fields from pharmaceutical to chemical industry (Figure 1.1). Biocatalysts have many important features, such as high chemoselectivity, regioselectivity and stereoselectivity at ambient temperatures[2]. Amongst biocatalysts, heme-containing cytochrome P450 (P450) oxygenases are a particularly attractive target because of their capability to catalyze oxidation of hydrocarbons with high efficiency and selectivity[3-5].

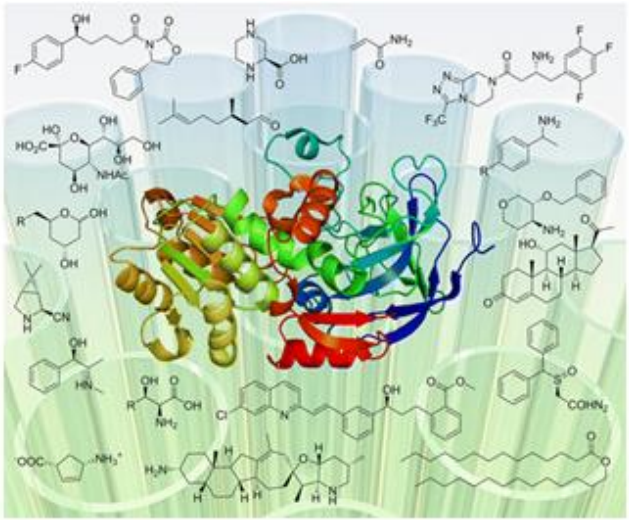

Figure 1.1. Structure of a biocatalyst and examples of their substrates
(Source: Torrelo et al., 2014)

1.2. Cytochrome P450 (P450) Oxygenases

Cytochrome P450 enzymes (CYP or P450) are monooxygenases that catalyze biologically important reactions with high efficiency and selectivity[6]. Their reactions consist of oxidation of different substrates shown in Figure 1.2. P450s catalyze the cleavage of bound molecular oxygen and formation of an oxygenated product as by using the heme prosthetic group(iron protoporphyrin IX,[3] Figure 1.3). Heme group is a porphyrin ring which has four pyrrole subunits connected by methine bridges, is a hydrophobic and planar molecule[7]. CYPs also catalyze other crucial reactions like hydroxylation, epoxidation, dealkylation, and reduction (Table 1.2.). These oxygenases participate in the metabolism of xenobiotics as a protective role, and biosynthesis of critical signaling molecules used for control of development and homeostasis[8].

P450 enzymes form a Fe(II)- CO complex which has a characteristic absorption spectrum (Soret band) near 450 nm, when bound to carbon monoxide[7], due to the cysteine thiolate residues of the protein[9]. P450s have thousands of potential substrates [10]. For example, they can participate in steroid anabolism or they can react in xenobiotic oxidation [10]. Some of the xenobiotics and their physiologically occurring compounds are shown in Table 1.1.

Figure 1.2. General reaction of P450s

Table 1.1. Some of the substrates for P450 enzymes (Source: Porter and Coon,1991)

XENOBIOTICS	PHYSIOLOGICALLY OCCURRING COMPOUNDS
Drugs, including antibiotics	Steroids
Carcinogens	Eicosanoids
Antioxidants	Fatty acids
Solvents	Lipid hydroperoxides
Anesthetics	Retinoids
Dyes	Acetone, acetol
Pesticides	
Petroleum products	
Alcohols	
Odorants	

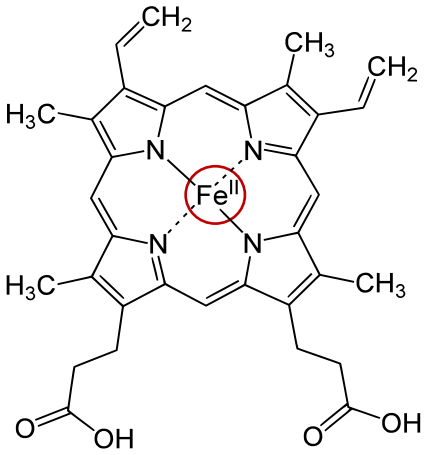

Figure 1.3. Structure of iron protoporphyrin IX

Table 1.2. Some reactions of the cytochrome P450s (Source: Koo et al., 2000; Sono et al., 1996)

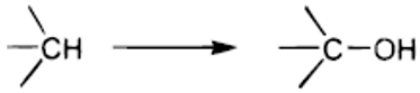	Hydrocarbon hydroxylation
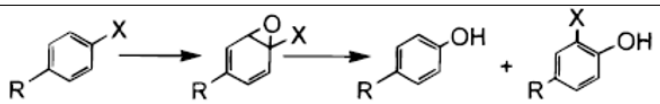	Arene epoxidation, aromatic hydroxylation
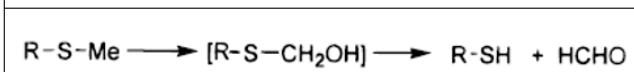	S-Dealkylation
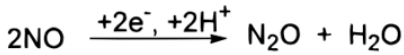	NO reduction

P450 reactions generally start with the transfer of electrons from NAD(P)H to either NADPH-cytochrome P450 reductase or a ferredoxin reductase[11]. This leads to the reductive activation of molecular oxygen followed by the insertion of one oxygen atom into the substrate[11]. There are two different pathways, monooxygenase and oxidase pathways, including catalyzed C-H oxidations of saturated hydrocarbons as seen Figure 1.4., and Figure 1.5., respectively[12]. In the monooxygenase pathway, an oxygen-atom are transfered by a metal center . In the oxidase pahtway O_2 is a proton or electron acceptor from reduced-metal center. In these patways the electrons are transferred from the metal to the oxidant. However, in nature Cytochrome P450 can play an important role in the electron transportation[12].

The first P450 was identified by Klingenberg et al. in 1958 from rat liver microsomes[13]. Nowadays, more than 300,000 members of the P450 family from all three domains, eukaryote, bacteria, and archaea are known[14-16].

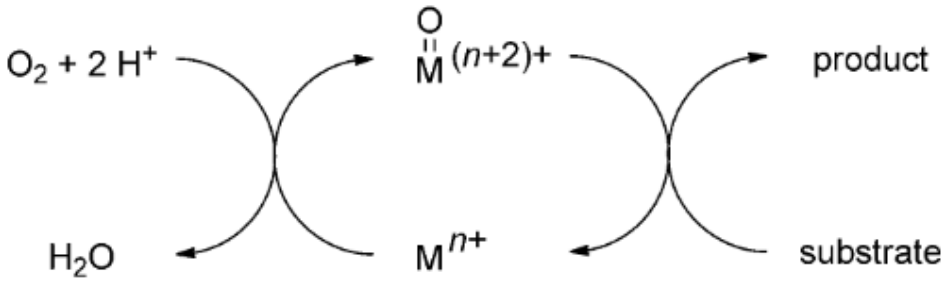

Figure 1.4. Monooxygenase pathway (Source: Roduner et al., 2013)

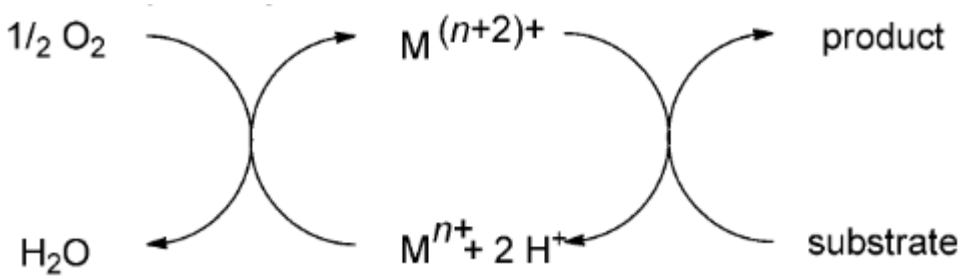

Figure 1.5. Oxidase pathway (Source: Roduner et al., 2013)

1.2.1. Importance of P450

P450s have important roles in biology, pharmaceutical industry, agriculture, biotechnology and even aesthetics[15]. P450s have high degrees of regio- and stereoselectivity which are important features in commercial applications, such as in the area of active pharmaceutical ingredient synthesis[7]. CYPs have a variety of medically important substrates including steroid hormones, prostaglandins, procarcinogens, and a range of pharmacological compounds[17]. Some bacterial P450s such as CYP105A3, which catalyze the hydroxylation of mevastatin to pravastatin, can be used in the pharmaceutical

industry (Figure 1.6). Pravastatin is a selective inhibitor (cholesterol absorption inhibitor) involved in cholesterol biosynthesis[7], it is used as a drug to treat low density lipoprotein cholesterol (LDL-cholesterol)[18].

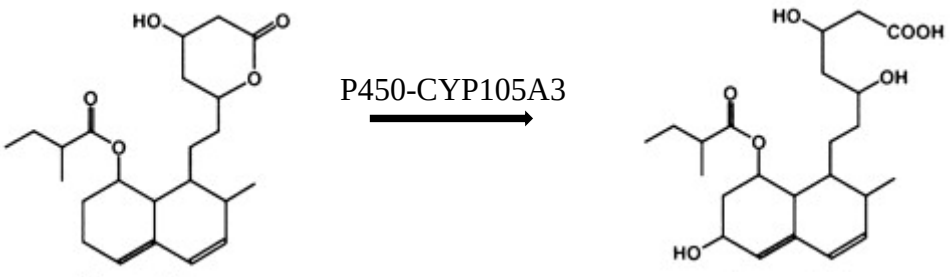

Mevastatin Pravastatin

Figure 1.6. Hydroxylation of mevastatin to pravastatin catalyzed by P450s[5]

1.2.2. The Thermophilic Cytochrome P450 119

CYP119 is a thermophilic P450 enzyme from an archaea called *Sulfolobus acidocaldarius.* Initially, the source of CYP119 was misidentified from an extreme acidothermophilic archaea *Sulfolobus solfataricus*[19]. However, Rabe et al. identified the correct CYP119 source as *Sulfolobus acidocaldarius* by PCR amplification with CYP119 specific primers. The *Sulfolobus acidocaldarius* is a sulfur-oxidizing organism, which grows in thermal acidic habitats (pH: 2.4 and temperature: 83°C) especially in Yellowstone National Park[20]. The electronmicrographs of thin sections of *S. acidocaldarius* and their habitat are shown in Figure 1.7 (A and B). The crystal structure of CYP119 was first determined by Yano et al.[5] and it was followed by an independent structure from Park et al.[21]. CYP119 has only 368 residues, which is one of the most distinctive feature that differentiates CYP119 from other P450s[22]. For example, P450cam or P450eryF have 414 and 403 residues, respectively; CYP119 has a shorter N-terminal segment and surface loops[5, 22]. The crystal structure of CYP119 is shown Figure 1.8. with the heme active site in the center of the CYP119. The heme active site contains

an iron ion surrounded by four nitrogen atoms and protoporphyrin IX cofactor in the center (Figure 1.9).

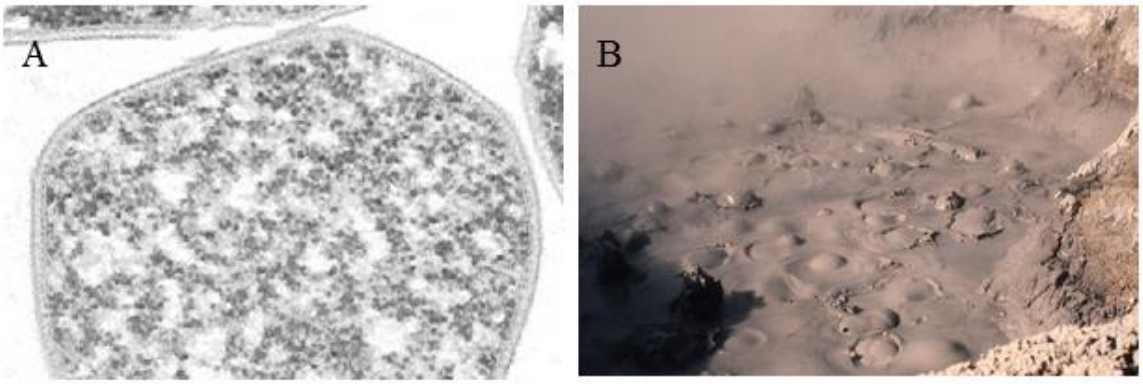

Figure 1.7. Electron micrographs of thermoacidophile *S. acidocaldarius* from NCBI genome project (A)[23] and their habitat in Yellowstone National Park (B)[24]

1.2.3. The CYP119 reactions

Although the natural substrates and oxygen partners of CYP119 are unknown, CYP119 can act on some artificial substrates and oxygen donors. CYP119 can catalyze different reactions such as oxidation of Amplex Red (Figure 1.10), epoxidation of styrene (Figure 1.11), hydroxylation of lauric acid (Figure 1.12), chemical dehalogenation, and electrochemical reduction of nitrite, nitric oxide, and nitrous oxide[25]. CYP119 can use hydrogen peroxide (H_2O_2), tertbutyl hydroperoxide (TBHP) and cumene hydroperoxide (CHP) as electron acceptors[25]. These oxidants are also suitable substitutes of the natural electron acceptors in the enzymatic reaction of P450 enzymes[25].

In this thesis; oxidation of Amplex Red and epoxidation of styrene were catalyzed with produced CYP119s in the presence of H_2O_2 and TBHP as oxygen acceptors, recpectively, in potassium phosphate buffer. The different conditions for these reactions were investigated.

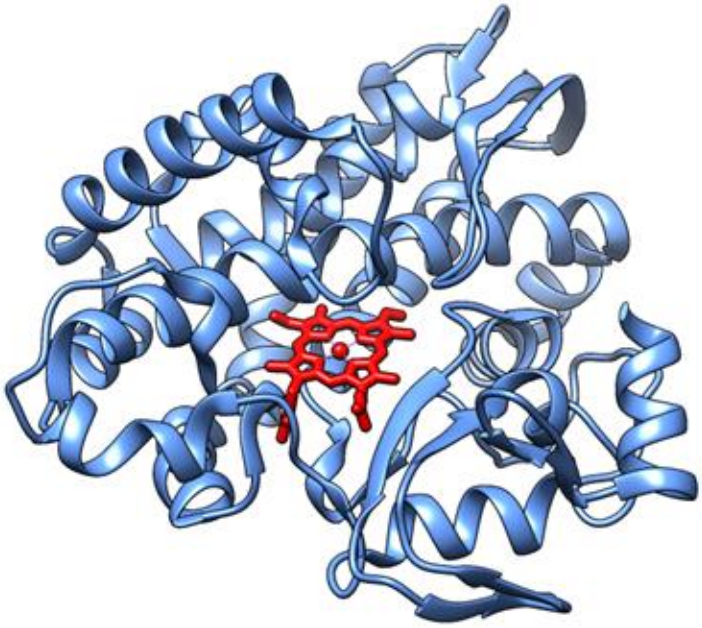

Figure 1.8. The crystal structure of CYP119 with the heme active (red) site in the center of the CYP119[26]. The illustration was produced with Chimera.
PDB ID: 1F4U[5]

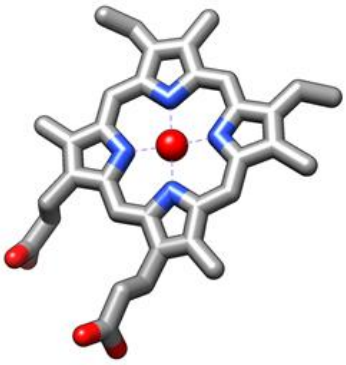

Figure 1.9. The heme active site of CYP119. Protoporphyrin IX (grey), nitrogens (blue) and iron ion (red) are shown. The illustration was produced with Chimera.

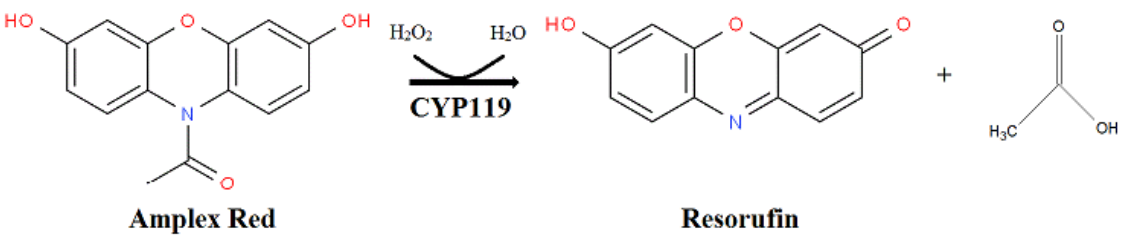

Amplex Red **Resorufin**

Figure 1.10. The Amplex Red reaction catalyzed by CYP119 using hydrogen peroxide as the oxygen donor[26]

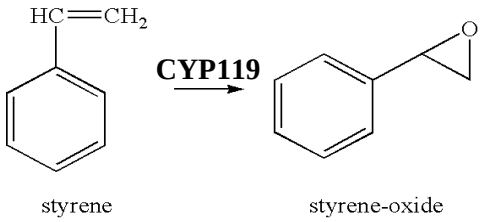

Figure 1.11. The styrene reaction catalysed by CYP119 using hydrogen peroxide as the oxygen donor

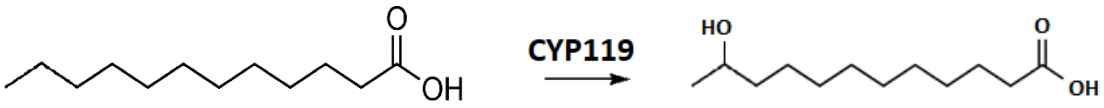

Figure 1.12. Hydroxylation of the lauric acid catalyzed by CYP119

1.3. The pET Cloning and Expression Systems

The pET Systems are one of the most powerful systems for the cloning and expression of recombinant proteins in suitable *E. coli* cells. A source of T7 RNA polymerases provide induction of protein expression in the host cells. Plasmids are transformed into expression hosts containing a chromosomal copy of the T7 RNA polymerase gene under lacUV5 control, and expression is induced by the addition of isopropyl β-D-1-thiogalactopyranoside (IPTG). T7 RNA polymerase is quite selective and active that almost all of the cell's resources are converted to target gene expression. The interested gene can comprise more than 50% of the total cell protein a few hours after induction. Figure 1.13 shows the pET cloning and expression systems components which are pET vector DNA, host bacterial strains such as BL21(DE3) and BL21(DE3) pLysS, induction control clone and glycerol stock.

δ-aminolevulinic acid (ALA) is the precursor for heme biosynthesis shown in Figure 1.14. The eight ALA molecules conjugate to yield protoporphyrin IX (PpIX) and finally it formates the heme structure[27]. In this thesis ALA and IPTG were optimized together to maximize protein expression.

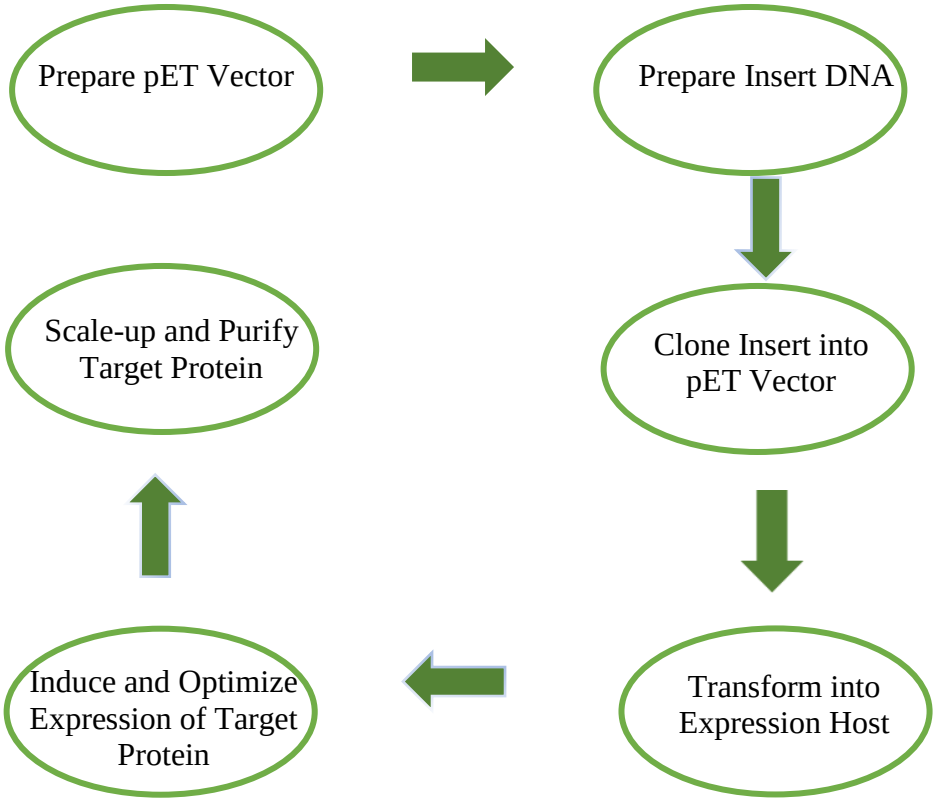

Figure 1.13. The pET cloning and expression system components

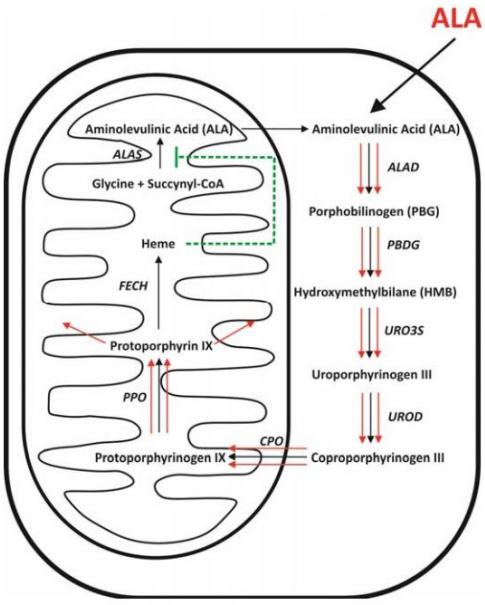

Figure 1.14. Heme biosynthesis started with the ALA molecule
(Source: Wachowska et al., 2011)

1.4. Polyhistidine Tag Protein Purification Systems and Advantages

Polyhistidine Tags (His-tags), which typically contain six or more consecutive histidine residues, are now commonly used in protein purification. His-tagged proteins are easily separated from the cell lysate by using immobilized metal affinity chromatography (IMAC). In IMAC, divalent cations (usually Ni^{2+}, Co^{2+}, Cu^{2+} or Zn^{2+}) are adhered to a solid matrix; around neutral pH the histidine residues form complexes with the chelated metal ions[28]. The protein of interest can then be eluted by displacement of histidine by addition of imidazole to the mobile phase or changing the pH of the solution. Since His-tags are relatively small in size (~2.5 kDa), they are thought to not affect the structure and function of proteins[29]. Yet, recent reports suggest that this assumption may be incorrect[30-32]. While the application of His-tags for protein purification has been extremely useful in increasing purity and yield of recombinant proteins, disregarding the consequences of His-tags on native protein structure and function will lead to non-reproducibility and confusion in literature[33]. Over 90% of recombinant proteins are purified using His-tags. Many times, the His-tags do not affect with the crystallization of proteins and they can even be acted in the formation of crystal contacts. In contrast, the B-factor, which acts the general displacement of atoms in a crystal structure, shows that the presence of a His-tag increases this value compared to structures determined without His-tag, thus making crystallization more difficult. This results also suggests that addition of a His-tag can alter protein dynamics and possibly impact protein activity or function[30].

1.5. Current Problems of P450 119 and Proposed Solutions

The first problems are about the low yield of thermophilic CYP119 and long prosess of expression of CYP119. For example, Yano et al. used a 40-liter fermenter to produce enough CYP119 for their crystallization work, and they were able to obtain CYP119, which was expressed during 36 hours after 2 overnigth growth[5]. Another study from McLean et al. showed that 64 liters culture of CYP119 was used to get sufficient

expressed CYP119 in a long step[3]. Expression conditions of CYP119 were optimized to eliminate these timing and low yield problems. These conditions were determined as use different expression times, temperatures, IPTG and ALA concentration and also different cells from the cloning petri. Thus, to increase the yield of CYP119 in shorter way was aimed in this study.

The second quite important problem of CYP119s is about isolation and purification steps. Isolation and purification CYP119s have difficult and time consuming steps when used (for being used) an ammonium sulfate precipitation or anion-exchange chromatography[3]. Anion-exchange chromatography separates molecules based on their net surface charge; however, it has also big and expensive systems. Another example, Koo et al. used ion exchange chromatography, dialyze, and equilibration column, one by one to purified to the CYP119[34]. They also used to remove the polybuffer by ammonium sulfate precipitation[34]. In this thesis, cloning of polyhistidine tags into CYP119 were planned to make easier and cheaper protein purification by using IMAC, which is a versatile methods. Here, IMAC was used to rapidly purify polyhistidine tagged CYP119 to enrichment CYP119 in a single purification step and His-tagged protein purities could be obtained up to 95% purity by IMAC in high yield.

IMAC is the most effective method to easly purify to His-tagged proteins. However, the His-tags effects on the structure and activitiy of CYP119 are not known. In this study, the effects of His-tags on the structure and activity of the CYP119 were investigated. His-tag region was cloned in the N- and C-terminals of the protein to get more stable and active CYP119.

Purification using polyhistidine tags has been performed with successfully using a number of expression systems, including *Escherichia coli*, which is the most basic system because of having short reproductivity time, *Saccharomyces cerevisiae*, mammalian cells, and baculovirus-infected insect cells.

In addition of IMAC systems, the heat prosess was used to enrichment to the CYP119. The heat treatment of purification method can help to obtain sufficient for tagged proteins expressed.

1.6. Aim of the Study

Initial scope of this study was optimization of recombinant production and purification of the thermophilic Cytochrome P450 119 (CYP119). Polyhistidine tags (His-tags) are commonly used to simplify protein purification. Here, CYP119 was expressed and purified though cloning of N-terminal and C-terminal His-tags (N-His-CYP119 and C-His-CYP119) under the optimum conditions. In addition, thermostabilities of the N-His-CYP119 and C-His-CYP119 were characterized and compared with Wild type CYP119 (Wt-CYP119). The Amplex Red oxidation efficiencies of optimally produced N-His-CYP119 and C-His-CYP119 with hydrogen peroxide (H_2O_2) were investigated at different temperatures and compared with the efficiency of Wt-CYP119. Also, epoxidation of styrene was catalysed by N-His-CYP119, at different temperatures, since it showed higher oxidation activity than C-His-CYP119. At the end of the study, impacts of N-terminal and C-terminal His-tags on the structure, function and stability of CYP119 were determined. This study aims to optimize expression and isolation of the thermophilic CYP119 enzyme and to determine oxidation reactions of His-tagged CYP119s in order to develop a stable and efficient biocatalyst for selective oxidation of hydrocarbons. This will lead to an increase in the production of this important enzyme which will increase the utilization of these enzymes in the industry. Besides, the effects of His-tags on the structure and activity of the CYP119s were investigated. These results showed that His-tags can influence enzyme mechanisms and one should be careful using His-tags especially in these studies.

CHAPTER 2

MATERIALS AND METHODS

2.1. Materials

The CYP119, different vectors and primers, compotent cells, enzymes, clean up kits, mediums, chemicals and equipments were used.

2.1.1. CYP119, Vectors and Primers

- The DNA CYP119 in pET-11a was a gift from Teruyuki Nagamune (Addgene library # 66131) (Appendix A)[35].
- The plasmids pET-14b with N-terminal Histidine tag (Appendix A) and pET-20b (+) with C-terminal Histidine tag (Appendix A).
- T7 universal primers

2.1.2. Cells Used, Enzymes, Clean up Kits and Mediums

- *E. coli* DH5α competent cells used for cloning. *E. coli* BL21(DE3) competent cells used for expression of the gene.
- *NdeI*, *BamHI* and *XbaI* restriction enzymes; T4 DNA Ligase; Alkaline Phosphatase, Calf Intestinal (CIP); Q5 Hot Start High-Fidelity 2X Master Mix; Q5 site directed mutagenesis kit (BioLabs).
- Macherey-Nagel Plasmid DNA purification kit.

- LB broth medium (10 g/L tryptone, 5 g/L yeast extract and 10 g/L NaCl) for cell growth. SOC medium (20 g of tryptone, 5 g of yeast extract, 0.5 g of NaCI, 10 ml of a 250 mM solution of KCl, 5 ml of a sterile solution of 2 M $MgCl_2$, 20 ml of a sterile 1 M solution of glucose; per liter at pH 7.0) for cell growth during transformation. 2xYT medium (16 g/L tryptone, 10 g/L yeast extract and 5 g/L NaCl at pH 6.8) broth for cell growth in a large scale. LB agar used for cell growth.

2.1.3. Chemicals and Equipments

Aminolevulinic acid (ALA), Ampicillin, DNA ladder, Isopropyl β-D-1-thiogalactopyranoside (IPTG), PageRuler™ Prestained Protein Ladder, Styrene, 50% sterile glycerol.

Centrifuge, Dry-bath, HPLC, pH meter, Nanodrop, Shaking incubator, Thermal cycle, UV-Vis spectrometers, Vario-scan, Vortex, Water-bath

Protein sequences (Wt-CYP119, N-His-CYP119, and C-His-CYP119) are shown Appendix B.

2.2. Cloning of His-tag into CYP119

Polyhistidine tags were cloned into the N-terminal and the C-terminal of CYP119 via plasmids pET14b and pET20b (+), respectively.

2.2.1. N-terminal His-tag Addition

The DNA coding CYP119 pET-11a was obtained from Teruyuki Nagamune (Addgene, #66131)[35]. pET-11a included CYP119 gene digested with polylinker region

with *NdeI* and *BamHI-HF* restriction enzymes (Table 2.1) at 37 °C for 30 minutes. The digested CYP119 loaded on a 1% of agarose gel. The digested DNA extracted from the gel.

pET-14b with N- terminal 6 histidine tags could not be digested with both enzyme due to restriction sites proximity in DNA sequence. The plasmid (pET-14b) was first digested with *BamHI-HF* restriction enzyme (Table 2.2) at 37 °C for 30 minutes and the digested DNA was cleaned up. The singly digested and cleaned plasmid was again digested with *NdeI* restriction enzyme (Table 2.3) at 37 °C for 2 hours and the double digested DNA was cleaned up. Double digested and cleaned pET-14b was de-phosphorylated with alkaline phosphatase enzyme at 37 °C for 30 minutes to avoid self-ligation of the plasmid and cleaned up. Components of de-phosphorylation of digested pET-14b are as seen in Table 2.4.

The DNA concentration of the de-phosphorylated double digested pET-14b and CYP119 extracted from the digestion gel were measured via nanodrop.

New England Biolabs' ligation calculation program was used to calculate the DNA concentration to ligate the digested gene and the plasmid (Table 2.5.). DNAs ligated ligated with 1 to 5 insert to vector ratio with T4 DNA ligase enzyme at 16℃ at overnight. Constructed CYP119+pET-14b transformed into *E. coli DH5α* competent cells. 5 colonies were chosen for colony Polymerase Chain Reaction (cPCR). Colony PCR was performed to select the recombinant colonies from the others. Selected colonies are dissolved in 0.1 ml sterile deionized water. 6 µl of dissolved cells were used for colony PCR. Rest of dissolved cells were stored at +4 °C in short time to grow if CYP119 amplified from these cells.

Primers were designed (Figure 2.6.) to amplify N-terminal His-tagged CYP119 from transformed plasmids. The PCR conditions for N-terminal His-tagged CYP119 are shown in Figure 2.7. The PCR products were loaded on 1% of agarose gel. The DNA CYP119 is 1107 base pairs. The PCR products visualisation showed that the three of DNAs amplified about 1000 bp. Dissolved cells stored at +4° C of amplified DNAs were grown in LB medium with 100 µg/ml concentration of ampicillin at 37℃ with 220 rpm shaking incubator for overnight. The plasmid DNAs were extracted from overnight cultures. The isolated DNAs were sequenced. Cloned CYP119 with N-terminal His-tag was conformed with DNA sequencing.

Table 2.1 Components of CYP119 digestion

Components	Volume
pET11a+CYP119	50 µl (7.6 µg)
10X cut smart	5 µl
NdeI	1 µl
BamHI -HF	1 µl
Total volume	57 µl

Table 2.2 Components of pET14b first digestion

Components	Volume
pET14b	50 µl (19,8 µg)
10x cut smart	5 µl
BamHI-HF	1 µl
Total volume	55 µl

Table 2.3 Components of pET14b second digestion

Components	Volume
pET14b	30 µl
10x cut smart	3 µl
NdeI	1 µl
ddH_2O	2.5 µl
Total volume	35 µl

Table 2.4 Components of dephosphorylation of digested pET14b

Components	Volume
pET14b	20 µl (5.3 mg)
10x cut smart	2 µl
CIP	1 µl
ddH_2O	2 µl
Total volume	25 µl

Table 2.5 Components of ligation of digested DNAs

Components	Volume
Pet14b	0,76 µl (86.48 ng)
Cyp119	5,56 µl (102.8 ng)
T4 ligase buffer	1 µl
T4 ligase	1 µl
Total volume	8,32 µl

Table 2.6. Primers designed to amplify CYP119 with N-terminal His-tag

Name (F/R)	Target-specific primer	Length	% GC	Tm	Ta
Forward Primer for CYP119 (CYP119 F)	GGAATTGTGAGCGGATAACAATTCCC	26 bp	46	58℃	49℃
Reverse Primer for CYP119 (CYP119 R)	TATCAGCGGCCGCTTCATTACTCTTCAAC	29 bp	48	62℃	

Table 2.7. PCR conditions for colony PCR

Step	Temperature	Time
Initial denaturation	98℃	30 seconds
	98℃	10 sec
Annealing (25 cycles)	49℃	10-30 seconds/kb
	72℃	20-30 second/kb
Final extension	72℃	2 minutes
Hold	4-10 ℃	∞

2.2.2. C-terminal His-tag Addition

CYP119 gene inside pET-11a plasmid and pET-20b (+) were digested with *XbaI* ve *BamHI* restriction enzymes (Table 2.8). The digested CYP119 and pET-20b (+) loaded on a 1% of agarose gel. The digested DNAs were extracted from the gel and purified via Macherey-Nagel Plasmid DNA purification kit. Double digested pET-20b (+) was de-phosphorylated with alkaline phosphatase enzyme to avoid self-ligation of the plasmid and purified. Components of de-phosphorylation of digested pET-20b (+) are shown in Table 2.9. DNA concentration of the de-phosphorylated double digested pET-20b (+) and CYP119 extracted from the gel were measured via nanodrop.

New England Biolabs' ligation calculation program was used to calculate the DNA concentration to ligate shown in Table 2.10. DNAs ligated with T4 DNA ligase enzyme at 16℃ at overnight. Constructed CYP119+pET-20b (+) was transformed into *E. coli* DH5α competent cells. 5 colonies were chosen for cPCR. Colony PCR was performed to verify the presence of the gene from the selected colonies. Selected colonies

were dissolved in 0.1 ml sterile deionized water. Here, a primer designed as the forward primer and the T7 reverse universal primer were used to amplify CYP119. The primers and PCR conditions are shown in Table 2.11 and Table 2.12., respectively. PCR products loaded on 1% of agarose gel. Amplified cells were grown in LB medium with 100 µg/mL concentration of ampicillin at 37℃ at 220 rpm in the shaking incubator for overnight. Plasmid DNAs were extracted from overnight cultures. The isolated DNAs were sequenced to confirm correct DNA's sequence.

After obtaining the correct CYP119+pET-20b DNA sequence, PCR was carried out to delete the stop codon that is between the gene and histidine tag with Q5 site directed mutagenesis kit (BioLabs). The interested DNA was exponentially amplified by PCR using the designed specific primers shown in Table 2.13. Q5 site directed mutagenesis components and conditions are shown in Table 2.14 and Table 2.15, respectively.

Table 2.8. Components of pET20b and CYP119 digestions

Components	**Volume**
pET11a DNA, pET 20b	10 µl (1.8 µg), (1.7 µg)
10X fast digest buffer	2 µl
XbaI	1 µl
BamHI	1 µl
ddH_2O	6 µl
Total volume	20 µl

Table 2.9. Components of dephosphorylation of digested pET20b

Components	**Volume**
pET20b DNA	18 µl (1.1 µg)
CIP	1 µl
Cut Smart buffer	2 µl
ddH_2O	9 µl
Total volume	30 µl

Table 2.10. Components of ligation of digested DNAs

Components	**Volume**
Vector	6.5 µl (203 ng)
Insert	7.5 µl (195 ng)
T4 Ligaz	1.5 µl
10X ligaz buffer	1 µl
Total volume	16.5 µl

Table 2.11. Primers designed to amplify CYP119 with C-terminal His-tag

Name (F/R)	Target-specific primer	Length	% GC	Tm	Ta
Forward Primer as CYP119_144 bp	AAGGCTTGAGGACCTAAG	18 bp	50	48˚C	49℃
T7 Terminal Primer	GCTAGTTATTGCTCAGCGG	29 bp	53	51˚C	

Table 2.12. PCR conditions for colony PCR

Step	Temperature	Time
Initial denaturation	98℃	30 seconds
	98℃	10 sec
Annealing (25 cycles)	49℃	10-30 seconds/kb
	72°C	20-30 second/kb
Final extension	72℃	90 sec
Hold	4-10 ℃	∞

Table 2.13. Designed primers for quick polymerase chain reaction

Name (F/R)	Target-specific primer	Length	% GC	Tm	Ta
Forward Primer	TCCGTCGACAAGCTTGCG	18 bp	61	53℃	65℃
Reverse Primer	TTCATTACTCTTCAACCTGACCAC	24 bp	42	54℃	

Table 2.14. PCR conditions

Step	Temperature	Time
Initial denaturation	98℃	30 seconds
	98℃	10 sec
Annealing (25 cycles)	65℃	10-30 seconds/kb
	72℃	20-30 second/kb
Final extension	72℃	2 minutes
Hold	4-10 ℃	∞

Table 2.15. KLD reactions mix

	25 µl RXN	Final concentration
Q5 Hot Start High-Fidelity 2X Master Mix	12.5 µl	1X
10 µM Forward Primer	1.25 µl	0.5 µM
10 µM Reverse Primer	1.25 µl	0.5 µM
Template DNA (1-25 ng/ µl)	1 µl	1-25 ng
Nuclease-free water	9.0 µl	

2.3. Optimization of Expression of CYP119 and Variants in *E. coli* Cells

After conformation of His-tagged CYP119 with DNA sequencing, the expression of CYP119 and variants were started into *E. coli* BL21(DE3) cells with using different parameters to obtain maximum protein yield. These parameters were different IPTG and ALA concentration, expression time, temperaures and colonies picked the petri.

2.3.1. Optimization of Production of Wild Type CYP119 (Wt-CYP119)

Wt-CYP119 in the plasmid pET-11a (without His-tag region) was transformed into the *E. coli* BL21 (DE3) bacteria by standard transformation methods. A single colony containing the plasmid and the gene (pET-11a-CYP119) was grown overnight in LB broth with 100 µg/ml ampicillin for expression of CYP119. Protein expression initiated by the addition of IPTG to the cells after the optical density at 600 nm of the cells reaches to optimum cell concentration about 0.8. Different IPTG concentration, expression time and temperature, and colonies were tested to achieve maximum the Wt-CYP119 expression.

2.3.2. Optimization of Production of C terminal His-tagged CYP119 (C-His-CYP119)

Constructed pET-20b (+) - CYP119 (with C-term His-tag region) transformed into the *E. coli BL21 (DE3)* bacteria by standard transformation methods. A single colony containing the plasmid and the gene (pET-20b (+)-CYP119) was grown overnight in LB broth with 100 μg/ml ampicillin for expression of CYP119. C-His-CYP119 protein expression initiated by the addition of IPTG to the cells after the optical density at 600 nm of the cells reaches to optimum cell concentration about 0.8. Several conditions were tested to achieve maximum expression of C-His-CYP119. These conditions were different IPTG and ALA concentrations, different expression times and temperatures and different cells picked from the transformation colonies.

2.3.3. Optimization of Production of N terminal His-tagged CYP119 (N-His-CYP119)

Constructed pET-14b- CYP119 (with N-term His-tag region) transformed into *E. coli BL21 (DE3)* bacteria by standard transformation methods. A single colony containing the plasmid and the gene (pET-14b-CYP119) was grown overnight in LB broth (medium containing 10 g/L tryptone, 5 g/L yeast extract, 10 g/L NaCl) with 100 μg/ml ampicillin for expression of CYP119. Protein expression initiated by the addition of IPTG to the cells after the optical density of the cells at 600 nm (OD_{600}) reaches to optimum cell concentration about 0.8. Several conditions were tested to achieve optimum expression of N-His-CYP119. These conditions were different IPTG concentrations, different expression times and temperatures and different cells picked from the transformation colonies.

2.4. Large Scale Expression both Cloned N-His-CYP119 and C-His-CYP119

N-His-CYP119 was expressed with under optimized conditions that are 0.3 mM ALA and 0.5 mM IPTG concentration at 8 hours at 30℃ in a 0.5 L 2xYT culture containing 100 μg/ml ampicillin. Expressed cells harvested with centrifugation at 3800 rpm at 30 minutes. Cell lysate was weighed about 2 g and frozen in -80 until isolation of protein.

C-His-CYP119 was expressed with under optimized conditions that are 0.5 mM ALA and 1 mM IPTG concentration at 16 hours at 30℃ in a 1 L 2xYT culture containing 100 μg/ml ampicillin. Expressed cells harvested with centrifugation at 3800 rpm at 30 minutes. Cell lysate was weighed about 4.5 g and frozen in -80 until isolation of protein.

2.5. Sodium Dodecyl Sulfate Polyacrylamide Gel Electrophoresis (SDS-PAGE) Analysis

Sodium Dodecyl Sulfate Polyacrylamide Gel Electrophoresis (SDS-PAGE) was first used to identify correct CYP119 protein band. Molecular weight of CYP119 is 43 kDa. Expression of CYP119 was monitored by SDS-PAGE. The differences of CYP119 expression, under different conditions, were determined.Isolation and purification steps of CYP119 were also observed by SDS-PAGE.

2.6. Isolation and Purification of N-His-CYP119 and C-His-CYP119

Isolation of His-tagged CYP119s were performed with a Nickel Nitrilotriacetic acid (Ni-NTA) affinity column. The frozen cells were first lysed in Buffer A (washing buffer), pH 7.5. The cells were sonicated 30 secs twice with 1 min interval and 15 sec once. The cell lysate was incubated at 65℃ for 1 h and centrifuged at 3800 rpm for 2

hours at 4 °C to remove all precipitating proteins. After some proteins and other cell contents completely precipitated, supernatant was taken to load the Ni-NTA column.

Ni-NTA column was washed with Buffer A, pH 7.5. Supernatants were loaded to the column. The protein-loaded column was then washed with 25-30 column volumes of Buffer A. CYP119 was eluted from the column with Buffer B (elution buffer), pH 7.5 and concentrated to < 2 ml. After concentration of the protein the buffer exchange was applied with Buffer C (desalting buffer) to removed salts and the protein was again concentrated < 1 ml. The buffers content is shown in Table 2.16.

Table 2.16. The buffers for protein isolation and purifications

Buffer A (washing buffer)	**Buffer B (elution buffer)**	**Buffer C (desalting buffer)**
50 mM phosphate buffer	50 mM phosphate buffer	50 mM phosphate buffer
150 mM NaCl	150 mM NaCl	20 mM NaCl
0.2 mM PMSF		5% glycerol
1 mM benzamidine HCl		
10 mM imidazole	150 mM imidazole	
pH 7.5	pH 7.5	pH 7.5

2.7. Thermostability Measurements of Wt-CYP119, N-His-CYP119, and C-His-CYP119

The thermostability of the N-His-CYP119 and C-His-CYP119 were tested and compared with the Wt-CYP119. Purified CYP119 variants were incubated in a dry-bath over a range of temperatures (25 °C, between 60 - 95 °C,) for 5 minutes in 50 mM potassium phosphate buffer, 7.4 pH. UV-Visible spectra of the enzymes in all temperatures were then taken between wavelengths of 350-650 nm. The difference spectra were obtained by subtraction of the spectrum at room temperature from the spectra obtained at higher temperatures. The shift in maximum Soret absorbance was monitored by ΔΔAbs(390-425) which was obtained by equation 1.

$$\Delta\Delta Abs(390\text{-}425) = \Delta Abs_{390nm} - \Delta Abs_{425nm} \quad (1)$$

Where ΔAbs is defined by the difference in absorbance at the specified wavelength observed at higher temperature compared to the absorbance at room temperature.

2.8. Testing the Activity of the Produced CYP119 Enzyme

CYP119 can catalyse some artificial substrates, although natural substrates of CYP119 is not known. Amplex Red and styrene were used as a substrate for the N-His-CYP119 and the C-His-CYP119. Amplex Red oxidation and styrene epoxidation were catalysed in the presence of hydrogen peroxide (H_2O_2) and tertbutyl hydroperoxide (TBHP) respectively, used as an oxygen donor. Also, Amplex Red oxidation was catalysed with Wt-CYP119 to compare with the His-tagged CYP119 activities.

2.8.1. Oxidation Reactions with Amplex Red

Reactions were performed with 10 μM Amplex Red and 1.5 mM H_2O_2 using both N- and C-His-CYP119 at different concentrations (1.5 μM; 2.5 μM, and 5 μM). Negative assay was only performed with enzyme and substrate without H_2O_2. Positive assays were performed with 1 unit of horseradish peroxidase (HRP) again with 1.5 mM H_2O_2, 10 μM Amplex Red. The experiments were done in duplicate. The product formation (Resorufin) was observed with fluorescence spectroscopy.

The same experimental conditions were used to carry out the Amplex Red oxidation using H_2O_2 at different concentrations to find the best H_2O_2 concentration required.

2.8.1.1. Kinetic Analysis of Amplex Red Reaction and Temperature Test

Amplex Red oxidations were followed during one hour at room temperature. The product formation was measured by fluorescence spectroscopy at emission of 580 nm and at exitation of 571 nm, after 1 min, 40 min, and 60 min of reactions. Amplex Red oxidations were also followed during two hours at 65 °C. A tube enzyme with H_2O_2 was heated to a separate tube with Amplex Red for 5 minutes at 65 ° C and then mixed and fluorescence measurements were taken.

The assays were performed with Wt-CYP119, N-His-CYP119 and C-His-CYP119. 1.5 μM enzyme, 1.5 mM H_2O_2 and 10 μM Amplex Red were used.

In addition, the effects of temperature on N-His-CYP119 stability were also tested by measuring its activity after incubation 90 °C. The N-His-CYP119 was heated during 10 minutes at 90 °C and cooled. The reaction was made with heated and cooled 1.5 μM N-His-CYP119 in the presence of 1 mM H_2O_2 and 10 μM Amplex Red. The product formation was followed with UV-Vis Spectroscopy at 571 nm. The control experiment was carried out with non-heated N-His-CYP119. Two reactions were compared to observe activity of N-His-CYP119 at 90 °C.

2.8.2. Epoxidation Reaction with Styrene

CYP119 also catalyses styrene epoxidation by CHP, H_2O_2 and TBHP as oxygen donors[25, 36]. The styrene epoxidation reactions were carried out by following the studies of Zhang et al.[36] with some modifications. The styrene (5 mM) catalysed with N-His-CYP119 (12,5 μM) in the presence of TBHP (5mM) in a 50 mM glycine buffer with pH 8.5. Styrene was catalysed by the N-His-CYP119 at room temperature and 65 °C to observe activity of high temperature. Styrene oxide (product) was monitored by High Pressure Liquid Chromatography (HPLC), after 10 minutes of the reaction. Here, Kinetex C18 column was used with using 30% ultrapure water and 70% acetonitrile as a mobil phase. Styrene and styrene oxide were analysed by their different retention times.

CHAPTER 3

RESULTS AND DISCUSSION

3.1. Results of Cloning of His-tagged CYP119

Polyhistidine tags (His-tags) were cloned into CYP119 using different plasmids to clone N-terminal and C-terminal His-tags. The constructed DNA with His-tags were sequenced to obtain correct sequence of N-His-tagged CYP119 (N-His-CYP119) and C-His-tagged CYP119 (C-His-CYP119).

3.1.1. Result of N-terminal His-tag Addition

CYP119 gene was successfully cloned into pET-14b plasmid with N-term His-tag. The digestion of CYP119-pET11a DNA and pET-14b DNA with N-term His-tag is shown Figure 3.1. The digested CYP119 and pET-14b were ligated via T4 ligase. The ligation product (including CYP119-pET-14b) was transformed into *E. coli* DH5α cells.

3.1.1.1. Colony PCR Results

After transformation of CYP119-pET-14b, colony PCR was made with CYP119 specific primers (Table 2.6.) to find correct colony including CYP119-pET-14b. The colony PCR products were loaded on a %1 agarose gel as seen in Figure 3.2. The correct N-term His-tagged CYP119 (N-His-CYP119) sequence is showed Appendix E. The DNA

of N-His-CYP119 was transformed into *E. coli* BL21(DE3) to test expression of CYP119 (Figure 3.3.).

3.1.2. Result of C-terminal His-tag Addition

CYP119 gene was successfully cloned into pET-20b (+) plasmid with C-term His-tag. Figure 3.4. is showing the digestion of CYP119 DNA and pET-20b (+) DNA. After digestion, the CYP119 and the plasmid were ligated via T4 ligase. The ligation product (including CYP119-pET-20b (+)) was transformed into *E.coli* DH5α cells.

3.1.2.1. Colony PCR Results

After transformation of CYP119-pET-20 (b), colony PCR was made with a specific primer and T7 reverse primer (Table 2.11.) to find correct colony including CYP119-pET-20b (+). The colony PCR products were loaded on a %1 agarose gel showing Figure 3.5. The correct C-term His-tagged CYP119 (C-His-CYP119) protein sequence showed Appendix F. The amplified CYP119's DNAs were transformed into *E.coli BL21(DE3)* to express the CYP119 (Figure 3.6.).

3.2. Optimization of Wt-CYP119 and Variants Protein Expression in *E. coli*

DNA of Wt-CYP119, N-His-CYP119 and C-His-CYP119 were transformed into *E. coli* BL21(DE3) cells to start expression test. The expression tests were optimized using different parameters that were expression temperatures and times, ALA and IPTG concentrations.

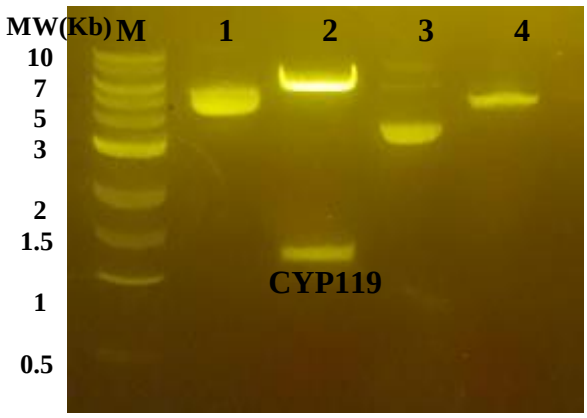

Figure 3.1. Double digestion of CYP119 and pET-14b (lane 2 and 4) and control DNA (lane 1 and 3) on 1% agarose gel. M. Molecular weight standards; 1. Uncut CYP119+pET-11a; 2. Digested CYP119 about 1100 bp; 3. Uncut pET-14b; 4. Digested pET-14b.

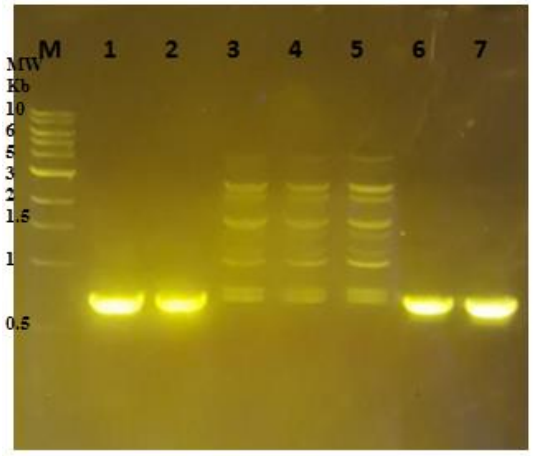

Figure 3.2. The colony PCR products of N-His-CYP119 with pET-14b in 1% agarose gel. M. Molecular weight standard; 1. Positive control, amplified CYP119 from pET-11a+CYP119; 2,6,7. Cloned CYP119s; 3-5 Noncloned CYP119s.

3.2.1. Optimization of Wt-CYP119 Protein Expression in *E. coli*

The Wild type CYP119 (Wt-CYP119) has a molecular weight of 43 kDa. The parameters tested of Wild type CYP119 expression to find optimum production of protein is shown in Table 3.1. The selected D and F colonies from the transformation petri gave the best expression result at 30 °C and 33-hour induction with 1 mM IPTG. The expression test was followed by 15% SDS-PAGE analysis as shown in Figure 3.7.

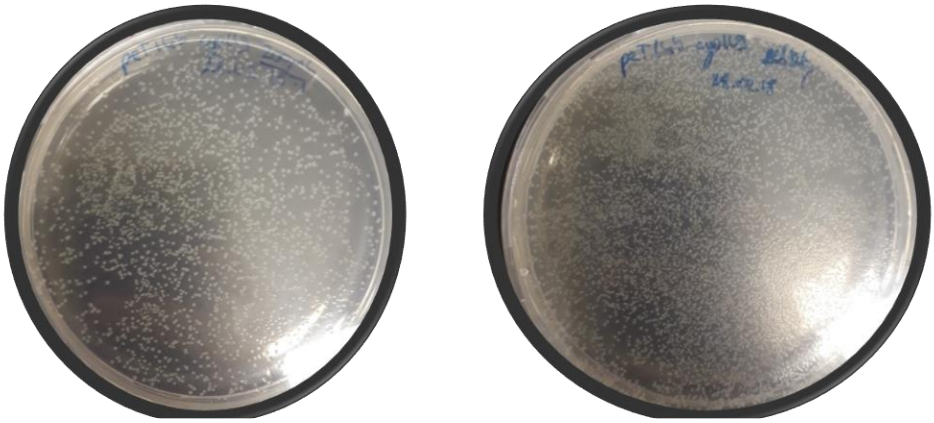

Figure 3.3. Colonies obtained in ampicillin containing plates after transformation of N-His-CYP119 DNA into the *E. coli BL21(DE3)* cells

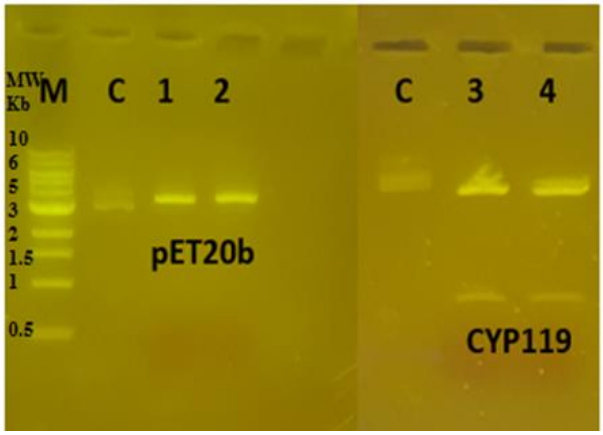

Figure 3.4. DNA electrophoresis of digested pET-20b (+) and CYP119. M. Molecular weight; C. Control, Uncut pET-20b (+) and pET-11a+CYP119, 1. and 2. Digested pET-20b (+) plasmid DNA (3516 bp), 3. and 4.: Digested pET-11a+CYP119 plasmid DNA (5700 bp and 1106 bp)

3.2.2. Optimization of C-His-CYP119 Protein Expression in *E. coli*

C-His-CYP119 were expressed with 0.3, 0.5 and 1 mM IPTG, in a period of 1-8-16-30 hours at 30 °C (Table 3.2.) The best conditions of C-His-CYP119 expression was found with 0.5 mM IPTG, 16-hour period and at 30℃ (Figure 3.9, lane 4). The SDS-PAGE analysis of C-His-CYP119 expression with 0.3 mM, 0.5 mM and 1 mM IPTG are showed that Figure 3.8, Figure 3.9, and Figure 3.10, respectively. The C-His-CYP119

were also expressed and purified from other *E.coli* proteins thanks to the heat treatment procedure with different time scales shown in Figure 3.11. The best induction time was found as 16 hours for C-His-CYP119 after the heat treatment analysis (Figure 3.11, lane 6). However, the 8 hours induction was also the best before the heat treatment (Figure 3.11, lane 2). Here, C-His-CYP119 may be degraded because of heating. The further investigation of expression of C-His-CYP119 was done with ALA and IPTG. The different ALA and IPTG concentrations were used to optimize their concentrations with for 16 hours induction at 30 °C. The best concentration of ALA and IPTG to express C-His-CYP119 are 0.5 mM ALA and 1 mM IPTG shown in Figure 3.12.

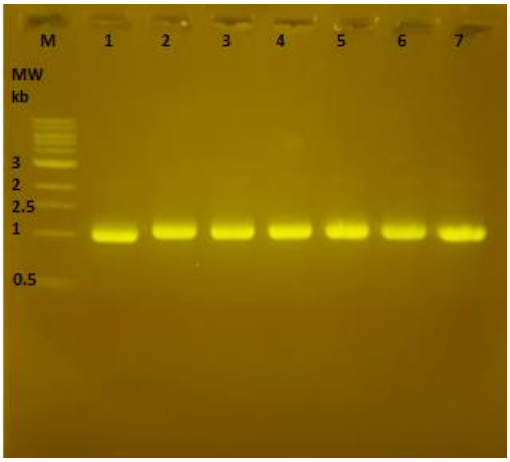

Figure 3.5. The colony PCR products of C-Term CYP119 with pET-20b (+) in 1% agarose gel. M. Molecular weight standard; 1. Positive control, amplified CYP119 from pET-11a+CYP119; 2-7. Cloned CYP119s into pET-20b (+)

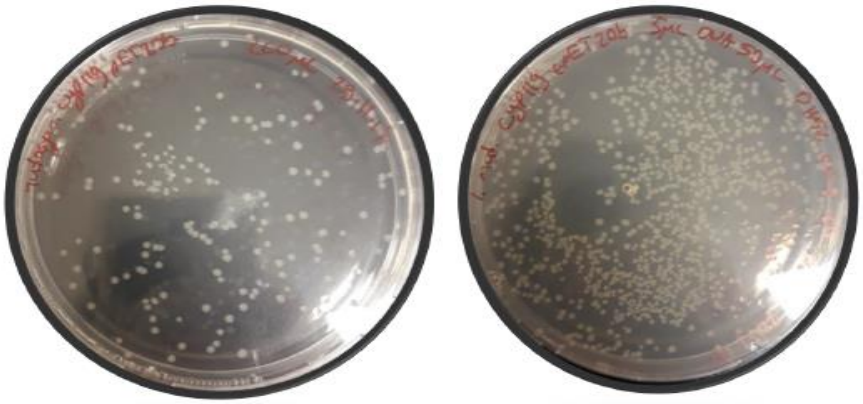

Figure 3.6. Colonies obtained in ampicillin containing plates after transformation of C-His-CYP119 DNA into the *E.coli* BL21(DE3*)* cells

Table 3.1. The conditions tested for Wt-CYP119 expression. The conditions of the expression test which marked* symbols are the best conditions of Wt-CYP119 expression (h: hour).

Chosen colonies	IPTG concentration (mM)	Induction time (h)	Induction temperature (°C)
A	0.5	1, 2, 5, 18	37
B	0.5, 1	1, 2, 5, 18, 33, 42	30, 37
C	0.5	1, 2, 5, 18	37
D*	0.5, 1*	1, 2, 5, 18, 33*, 42	30, 37
E	1	18, 33, 42	30, 37
F*	1*	18, 33*, 42	30, 37

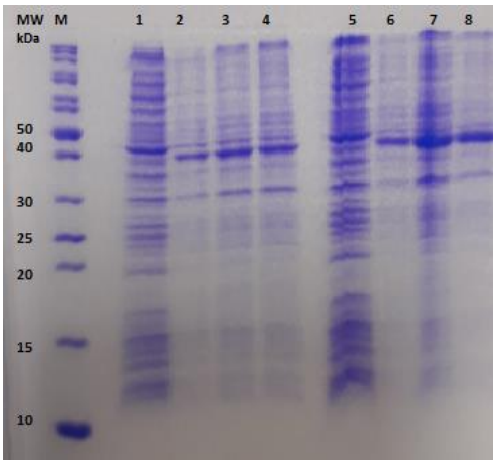

M. PageRuler™ Prestained Protein ladder
1. CYP119 D cells with no IPTG, 43 kDa
2. CYP119 D cells with 1 mM IPTG after 18 h
3. CYP119 D cells with 1 mM IPTG after 33 h
4. CYP119 D cells with 1 mM IPTG after 42 h
5. CYP119 F cells with no IPTG, 43 kDa
6. CYP119 F cells with 1 mM IPTG after 18 h
7. CYP119 F cells with 1 mM IPTG after 33 h
8. CYP119 F cells with 1 mM IPTG after 42 h

Figure 3.7. SDS-PAGE analysis of expression of Wt-CYP119 with 1 mM IPTG at 30°C. Molecular weight of Wt-CYP119 is 43 kDa.

Table 3.2. The conditions for C-His-CYP119 expression test (h: hour). The conditions for the expression test which marked * symbols are the best tested conditions

Chosen cells	IPTG concentration (mM)	Induction time (h)	Induction temperature (°C)
A*	0.3, 0.5*, 1	1, 8, 16*, 30	30*
B*	0.3, 0.5*, 1	1, 8, 16*, 30	
C	0.3, 0.5, 1	1, 8, 16, 30	
D	0.3, 0.5, 1	1, 8, 16, 30	

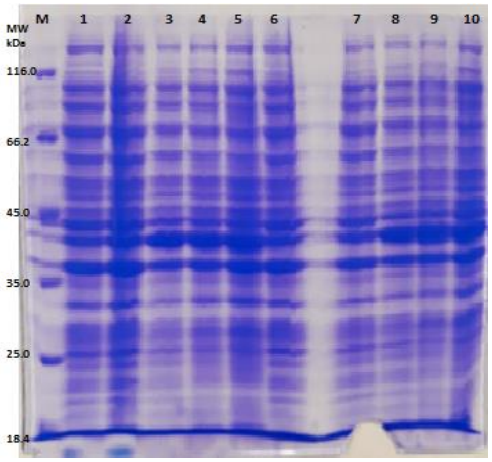

M. PageRuler™ Prestained Protein Ladder
1. CYP119 A cells with no IPTG
2. CYP119 A cells with IPTG after 1 h
3. CYP119 A cells with IPTG after 8 h
4. CYP119 A cells with IPTG after 16 h
5. CYP119 A cells with IPTG after 30 h
6. CYP119 B cells with no IPTG
7. CYP119 B cells with IPTG after 1 h
8. CYP119 B cells with IPTG after 8 h
9. CYP119 B cells with IPTG after 16 h
10. CYP119 B cells with IPTG after 30 h

Figure 3.8. SDS-PAGE analysis of the expression of C-His-CYP119 with 0.3 mM IPTG at 30°C. Molecular weight of C-His-CYP119 is about 43 kDa.

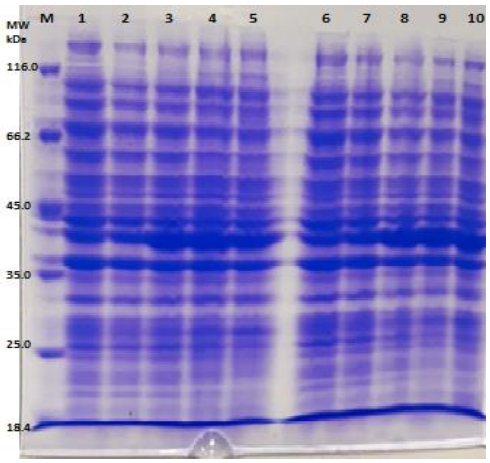

M. PageRuler™ Prestained Protein Ladder
1. CYP119 A cells with no IPTG
2. CYP119 A cells with IPTG after 1 h
3. CYP119 A cells with IPTG after 8 h,
4. CYP119 A cells with IPTG after 16 h
5. CYP119 A cells with IPTG after 30 h,
6. CYP119 B cells with no IPTG
7. CYP119 B cells with IPTG after 1 h,
8. CYP119 B cells with IPTG after 8 h
9. CYP119 B cells with IPTG after 16 h
10. CYP119 B cells with IPTG after 30 h

Figure 3.9. SDS-PAGE analysis of the expression of C-His-CYP119 with 0.5 mM IPTG at 30°C. Molecular weight of C-His-CYP119 is about 43 kDa.

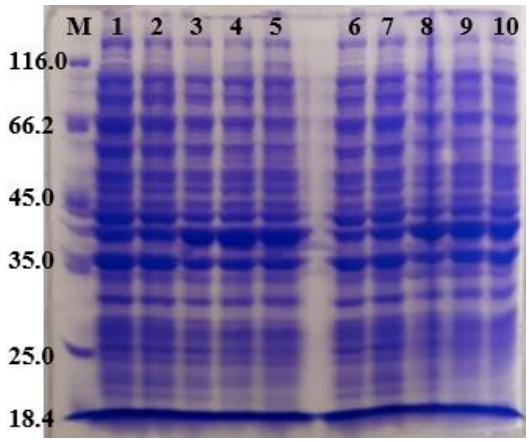

M. PageRuler™ Prestained Protein Ladder
1. CYP119 A cells with no IPTG
2. CYP119 A cells after 1 h induction
3. CYP119 A cells after 8 h induction
4. CYP119 A cells after 16 h induction
5. CYP119 A cells after 30 h induction
6. CYP119 B cells with no IPTG
7. CYP119 B cells after 1 h induction
8. CYP119 B cells after 8 h induction
9. CYP119 B cells after 16 h induction
10. CYP119 B cells after 30 h induction

Figure 3.10. SDS-PAGE analysis of the expression of C-His-CYP119 with 1 mM IPTG at 30 °C. Molecular weight of C-His-CYP119 is about 43 kDa.

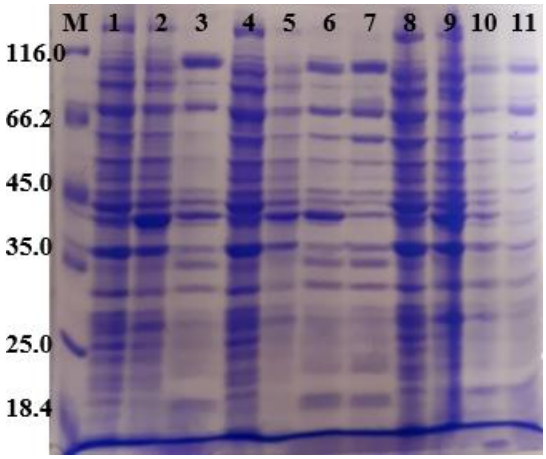

M. PageRuler™ Prestained Protein Ladder
1,4,8. CYP119 cells with no IPTG
2. CYP119 cells with IPTG after 8 h induction
3. CYP119 cells with IPTG after 8 h induction and heat treatment
5. CYP119 cells with IPTG after 16 h induction
6. CYP119 cells with IPTG after 16 h induction and heat treatment
7. CYP119 cells with no IPTG after 16 h induction and heat treatment
9. CYP119 cells with IPTG after 30 h induction
10. CYP119 cells with IPTG after 30 h induction and heat treatment
11. CYP119 cells with no IPTG after 30 h induction and heat treatment

Figure 3.11. Gel electrophoretic analysis of the expression of C-His-CYP119 throughout 8, 16 and 30 hours. Molecular weight of C-His-CYP119 is about 43 kDa.

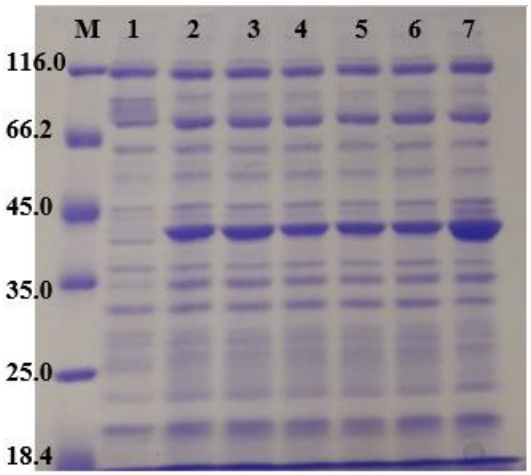

M. PageRuler™ Prestained Protein Ladder
1. CYP119 cells with no IPTG
2. CYP119 cells expression with 0.3 mM ALA and 0,3 mM IPTG
3. CYP119 cells expression with 0.5 mM ALA and 0,3 mM IPTG
4. CYP119 cells expression with 0.3 mM ALA and 0,5 mM IPTG
5. CYP119 cells expression with 0.5 mM ALA and 0,5 mM IPTG
6. CYP119 cells expression with 0.3 mM ALA and 1 mM IPTG
7. CYP119 cells expression with 0.5 mM ALA and 1 mM IPTG

Figure 3.12. SDS-PAGE analysis of the expression of C-His-CYP119 with different ALA and IPTG concentrations for 16 hours induction at 30 °C. Molecular weight of C-His-CYP119 is about 43 kDa.

3.2.3. Optimization of N-His-CYP119 Protein Expression in *E. coli*

N-His-CYP119 was expressed with 0.3 mM, 0.5 mM and 1 mM IPTG, for 1-8-16-30 hours at 30 °C (Table 3.3). The SDS-PAGE analysis of N-His-CYP119 expression with 0.5 mM IPTG showed optimum expression as seen in Figure 3.13. The N-His-

CYP119 showed no induction with 0.3 mM and 1 mM IPTG. The best time for induction was found 8 hours (Figure 3.13, lane 3 and lane 8).

Table 3.3. The condition of N-His-CYP119 expression test (h: hour). The conditions of the expression test which marked * symbols are the best tested conditions

Chosen cells	IPTG concentration (mM)	Induction time (h)	Induction temperature (°C)
A	0.3, 0.5, 1	1, 8, 16, 30	30
B	0.3, 0.5, 1	1, 8, 16, 30	30
C*	0.3, 0.5, 1	1, 8*, 16, 30	30*
D*	0.3, 0.5, 1	1, 8*, 16, 30	30*

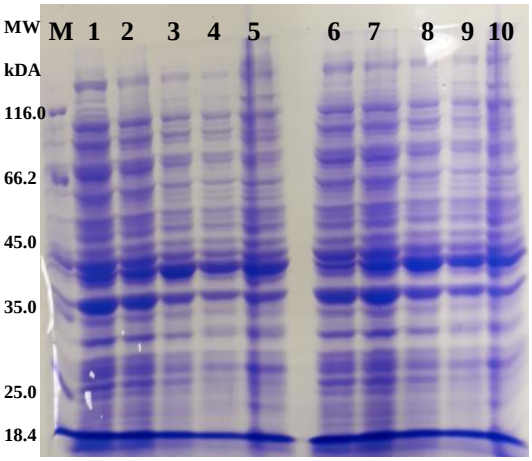

M. PageRuler™ Prestained Protein Ladder
1. CYP119 C cells with no IPTG, 43 kDa
2. CYP119 C cells after 1 h induction,
3. CYP119 C cells after 8 h induction
4. CYP119 C cells after 16 h induction
5. CYP119 C cells after 30 h induction
6. CYP119 D cells with no IPTG, 43 kDa
7. CYP119 D cells after 1 h induction
8. CYP119 D cells after 8 h induction
9. CYP119 D cells after 16 h induction
10. CYP119 D cells with after 30 h induction

Figure 3.13. Gel electrophoretic analysis of the expression of N-His-CYP119 with 0.5 mM IPTG at 30℃. Molecular weight of C-His-CYP119 is about 43 kDa.

3.2.4. Isolation and Purification of C-His-CYP119 and N-His-CYP119

After a 0.5 L protein expression, approximately 1.5 g and 2 g of C-His-CYP119 and N-His-CYP119 were obtained, respectively, in harvested *E.coli* BL21(DE3) cells. The final concentration and yield of the purified protein were 40.3 μM and 1.44 mg, respectively for C-His-CYP119. SDS-PAGE analysis of samples from each purification step is shown in Figure 3.14.

The final concentration and yield of the purified N-His-CYP119 were 100 μM and 4.8 mg, respectively. SDS-PAGE analysis of samples from each purification step is shown in Figure 3.15. Purification involved initial heat treatment of cell lysate at 65°C for 1 hr. This was followed by IMAC, which led to approximately 95% purity for both proteins. The heme incorporation of isolated proteins were observed by the absorbance ratio of 280 nm vs Soret (415 nm) absorbance, this ratio was 0.46 and 0.58 for N-His-CYP119 and C-His-CYP119, respectively; showing appropriate levels of heme incorporation for both proteins.

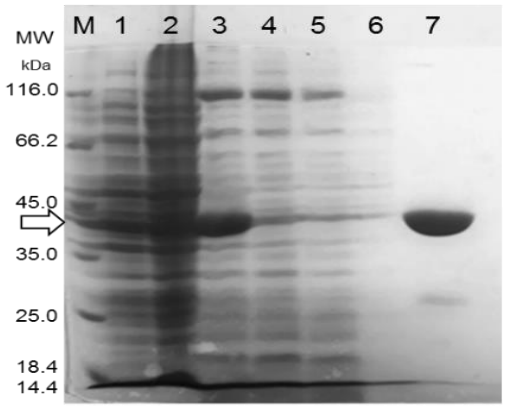

M. Molecular weight
1. Cell lysate
2. Pellet after heat treatment
3. Supernatant after heat treatment
4. Flow through
5. Wash 1
6. Wash 2
7. Purified protein

Figure 3.14. The SDS-PAGE analysis of C-His-CYP119 during the isolation and purification steps. C-His-CYP119 is about 43 kDa showing the arrow.

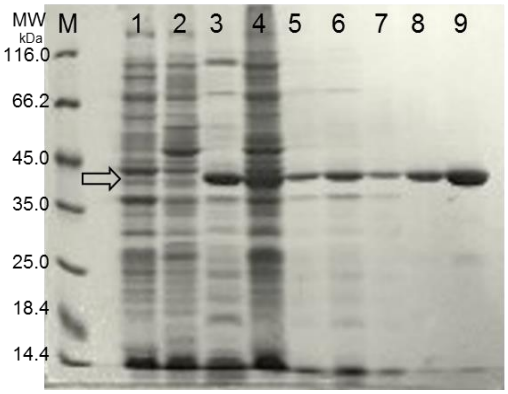

M. Molecular weight
1. Cell lysate before induction
2. Cell lysate after induction
3. Supernatant after heat treatment
4. Pellet after heat treatment
5. Flow through
6. Wash 1
7. Wash 2
8. Wash 3
9. Purified protein

Figure 3.15. The SDS-PAGE analysis of N-His-CYP119 during the isolation and purification steps. N-His-CYP119 is about 43 kDa showing the arrow.

3.3. Comparison of Spectroscopic Analysis of C-His-CYP119 and N- His-CYP119 with Wt-CYP119

The optical spectra of Wt-CYP119, N-His-CYP119 and C-His-CYP119 as isolated are shown in Figure 3.16. Wt-CYP119 shows maximum Soret absorbance at 414 nm and split α/β bands in 531 and 564 nm, similar to previously reported spectra [3]. Addition of histidine tag to N-terminal and C-terminal of the protein resulted in a small shift in the Soret maximum to 418 nm, while modest splitting of the alpha-beta (α/β) region was observed (Figure 3.16).

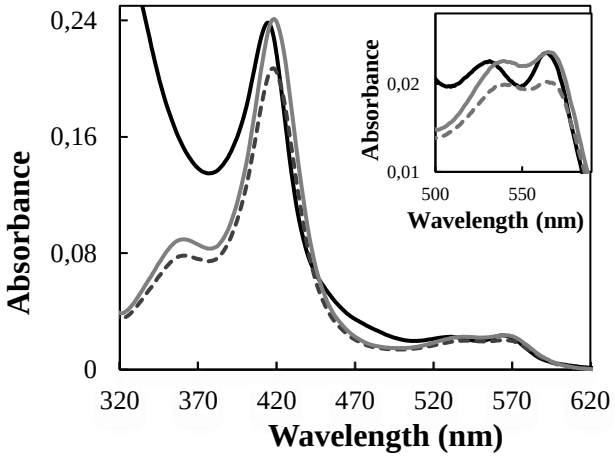

Figure 3.16. The comparison of UV-visible spectra of C-His-CYP119 (grey) and N-His-CYP119 (dash) with Wt-CYP119 (black). Inset: The changes observed in the α/β bands.

3.4. Changes in UV-Visible Spectra of C-His-CYP119 and N-His- CYP119 and Comparison with Wt-CYP119

The changes in UV-Visible spectra of Wt-CYP119, N-His-CYP119, and C-His-CYP119 are shown in Figure 3.17. The maximum Soret absorbance of Wt-CYP119 does not change with temperature up to the highest temperature tested (95°C) (Figure 3.17A). On the other hand, maximum Soret absorbance of C-His-CYP119 shifted to 415 nm with

increasing temperature up to 60 °C (Fig. 3.17C). In addition, there was a 12 % decrease in Soret absorbance of C-His-CYP119 from room temperature to 95°C. The maximum Soret absorbance of N-His-CYP119 also shifted to 415 nm when the temperature reached 90 °C; for N-His-CYP119 there was a 40% decrease in Soret absorbance at 95°C (Figure 3.17C).

The changes in the UV-Visible spectra were also monitored with increasing temperature for N-His-CYP119. A shift in maximum Soret absorbance of N-His-CYP119 from 418 to 415 nm was observed with increasing temperature (Figure 3.17B). In addition, N-His-CYP119 shows high activity at 65 °C; therefore, the decrease in Soret absorbance is not due to loss of the heme cofactor but a most likely a change in the electronic properties of the heme. The shift in Soret absorbance can be more clearly monitored by following the change in the difference in absorbance at 390 nm and 425 nm [ΔΔAbs(390 - 425)] (Figure 3.17D). Previous studies have shown an increase in high spin state for Wt CYP119 with increase in temperature. In accordance to previous results the ΔΔAbs(390 -425) for Wt-CYP119 increases with temperature. However, as seen in Figure 3.17D, N-His-CYP119 shows significantly higher shift in absorbance compared to Wt CYP119. Showing that the His-tag effected electronic properties of the active site heme.

3.5. Testing the Activity of the Produced CYP119 Enzyme

Activity of N-His-CYP119 and C-His-CYP119 were tested using different substrates and oxidants. Product formation was followed by fluorescence spectroscopy and UV-visible spectroscopy. These activities of were N-His-CYP119 and C-His-CYP119 compared to Wt-CYP119.

3.5.1. Fluorescence Spectroscopy Results of Amplex Red Reaction

The oxidase activity of Wt-CYP119 was investigated by following oxidation of Amplex Red by H_2O_2[25]. The product resorufin can be observed by fluorescence with excitation at 570 nm and emission at 585 nm. The excitation and emission spectra of the

reaction mixture containing 1.5 mM H_2O_2 and 10 μM Amplex Red with 1.5 μM Wt-CYP119 is shown in Figure 3.18, the spectra clearly show resorufin formation. Amplex Red oxidation of both N-His-CYP119 and C-His-CYP119 were performed using different concentration of the enzymes. The best product formation was achieved with N-His-CYP119 (Figure 3.19). Product formation is almost the same in experiments with N-His-CYP119 at different concentrations. In experiments with C-His-CYP119 at different concentrations, the concentration of the enzyme marked a reduction in the formation of residual products. The best reaction conditions were with 1.5 μM enzyme. The reason of the activity decreasing with increasing enzyme concentration may be due to the complexity of Amplex Red oxidation[37]. Positive control had a high amount of product formation observed when compared with activities of the CYP119 variants.

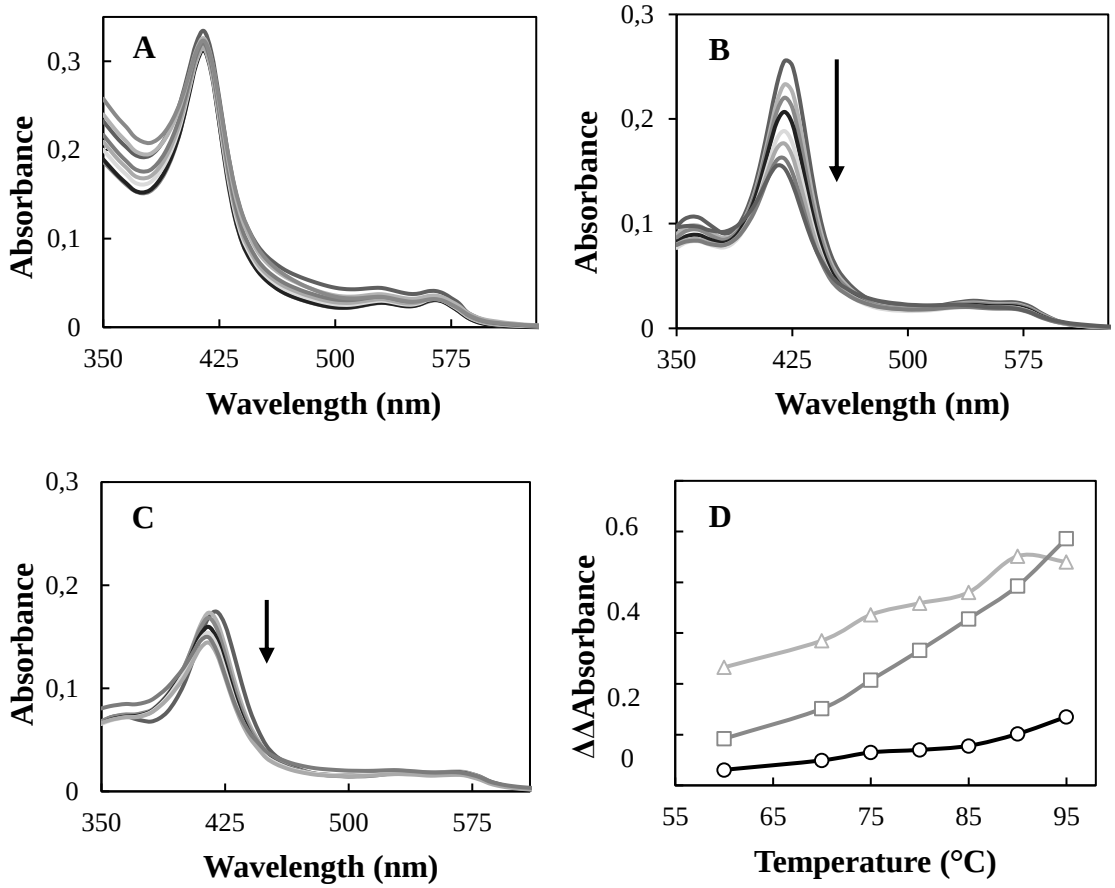

Figure 3.17. UV-Visible spectra of thermostability analysis of 3.5 μM Wt-CYP119 (A), 2 μM N-His-CYP119 (B) and 1.4 μM C-His-CYP119 (C). Spectra were taken at different temperature (RT: room temperature, 60, 70, 75, 80, 85, 90, and 95°C) after incubation for 5 minutes in 50 mM potassium phosphate buffer at pH 7,4. The normalized ΔΔAbs(390 -425) for C-His-CYP119 (□) and N-His-CYP119 (□), and Wt-CYP119 (□)with respect to the temperature increase from 25 °C to 95 °C (D).

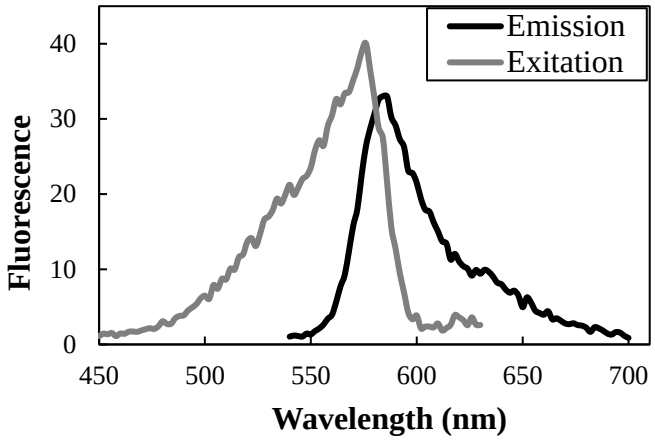

Figure 3.18. The excitation (black) and emission (grey) fluorescence of the Amplex Red oxidation product (resorufin) catalyzed by Wt-CYP119. Reaction components were 10 µM Amplex Red, 1.5 mM H_2O_2 and 1.5 µM Wt-CYP119 in 50 mM sodium phosphate at room temperature at pH 7.4; spectra taken after 40 minutes.

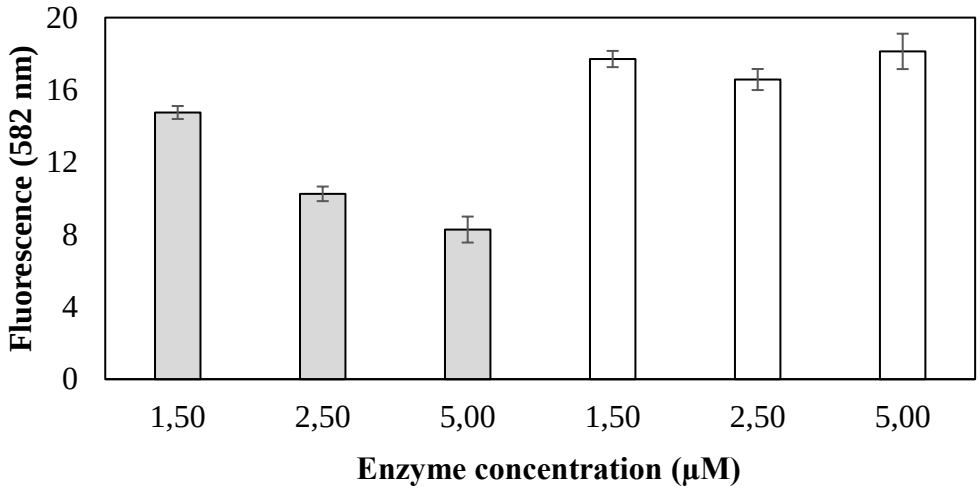

Figure 3.19. The Amplex Red oxidation of C-His-CYP119 (grey column) and N-His-CYP119 (white column) at different concentration. 582 nm is showing the product (resorufin) peak of Amplex Red oxidation after 2 minutes of reaction. The reaction was carried out with 10 µM Amplex Red, 1.5 mM H_2O_2 and enzyme in a sodium phosphate buffer, pH, 7,4, at room temperature.

Amplex Red reactions of both N-His-CYP119 and C-His-CYP119 were done using different concentration of H_2O_2. The best product formation was achieved with 2 mM and 1.5 mM H_2O_2 in the presence of C-His-CYP119, N-His-CYP119, respectively. (Figure 3.20). Here, N-His-CYP119 is more active than the C-His-CYP119 at different H_2O_2 concentrations. N-His-CYP119 showed 2.5-fold more activity than C-His-CYP119 in the presence of 1.5 mM H_2O_2 (Figure 3.20.).

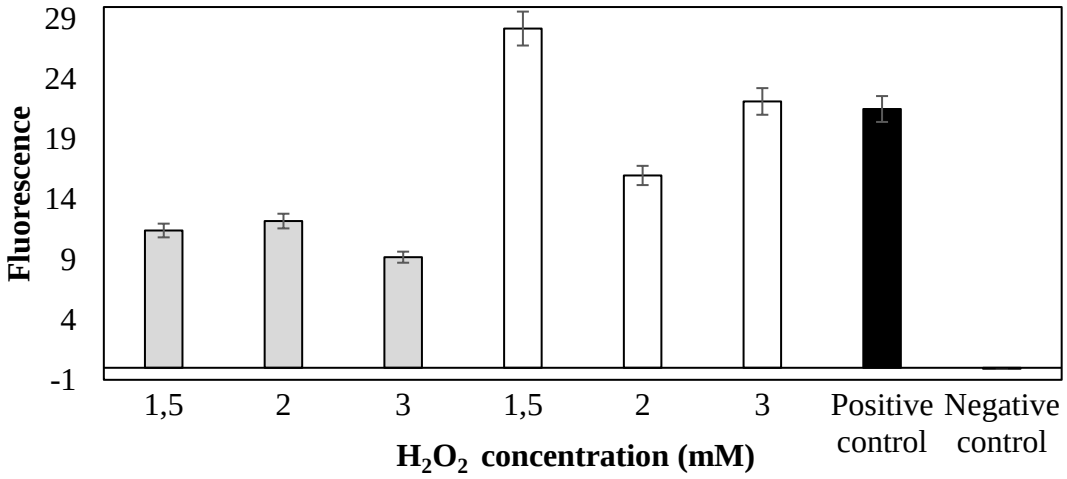

Figure 3.20. The Amplex Red oxidation of C-His-CYP119 (grey column) and N-His-CYP119 (white column) at different concentration of H_2O_2. Positive control (×0.025) 570 nm is showing the product (resorufin) peak of Amplex Red oxidation after 2 minutes of reaction. The reaction was carried out with 10 μM Amplex Red, 1.5 μM enzyme and H_2O_2 in a sodium phosphate buffer, pH, 7.4, at room temperature.

3.5.2. UV-Visible Spectroscopy Results of Amplex Red Oxidation

The fluorescence spectroscopic analyses of Amplex Red oxidation showed that the most suitable conditions of Amplex Red oxidation were with 10 μM Amplex Red 1.5 mM H_2O_2 and 1.5 μM N-His-CYP119 in sodium phosphate buffer, pH 7.4, at room temperature. N-His-CYP119 showed higher activity than C-His-CYP119. For that reason, the Amplex Red oxidation was carried out with 10 μM Amplex Red 1.5 mM H_2O_2 and 1.5 μM N-His-CYP119 in sodium phosphate buffer, pH 7.4, at room temperature to follow the product formation with UV-Vis spectroscopy.

The Amplex Red (10 μM) reactions were catalyzed by N-His-CYP119 (1.5 μM) in the presence of 1.5 mM H_2O_2 in sodium phosphate buffer, pH 7.4, at room temperature. Positive assays were performed with 1unit of Horseradish peroxidase (HRP) again with 1.5 mM H_2O_2, 10 μM Amplex Red in sodium phosphate buffer, pH 7.4, at room temperature. Negative control was carried out without the H_2O_2. The full spectrum after the reaction was measured between 370 nm and 650 nm (Figure 3.21). The product formation (resorufin) was observed in the UV-Visible spectra at 570 nm after the reactions as seen in Figure 3.21.

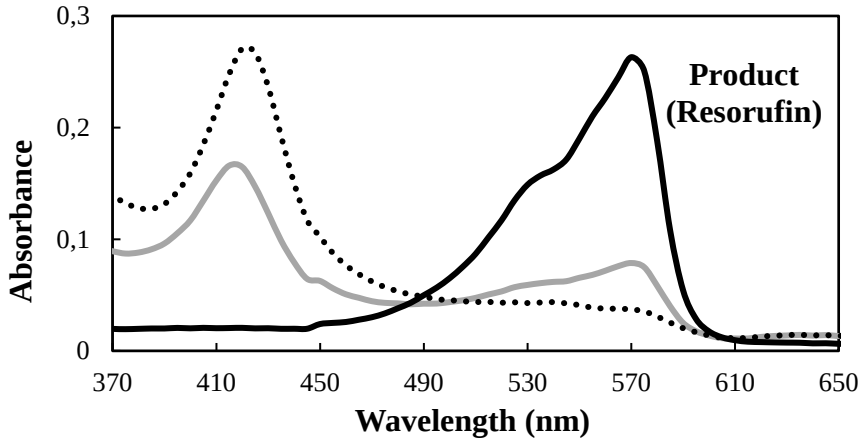

Figure 3.21. The UV-visible spectra of Amplex Red oxidation catalyzed by N-His-CYP119(grey), positive assay (black), and negative assay (dash).

3.5.3. Kinetic Analysis of Amplex Red Reaction and Temperature Test Results

The kinetic analyses of Amplex Red oxidation at room temperature and 65 °C are shown in Figure 3.22. Reaction was completed in 40 minutes at room temperature. The reaction was followed at room temperature and at 65°C to understand the effects of temperature on enzyme activity. As seen in Figure 3.22 Wt-CYP119 and N-His-CYP119 showed similar product formation at room temperature, while C-His-CYP119 showed only 20% of Wt-CYP119 activity. Increasing the temperature to 65°C results in an 80% decrease in the final yield for Wt-CYP119, however for N-His-CYP119 this decrease is

only 33%, and for C-His-CYP119 almost no decrease in activity is observed. From Figure 3.22, the observed rate constant for the formation resorufin at 65°C was determined to be 5.2×10^{-3} s^{-1}, 1.0×10^{-3} s^{-1}, 1.0×10^{-2} s^{-1} for Wt-CYP119, N-His-CYP119, and C-His-CYP119; respectively.

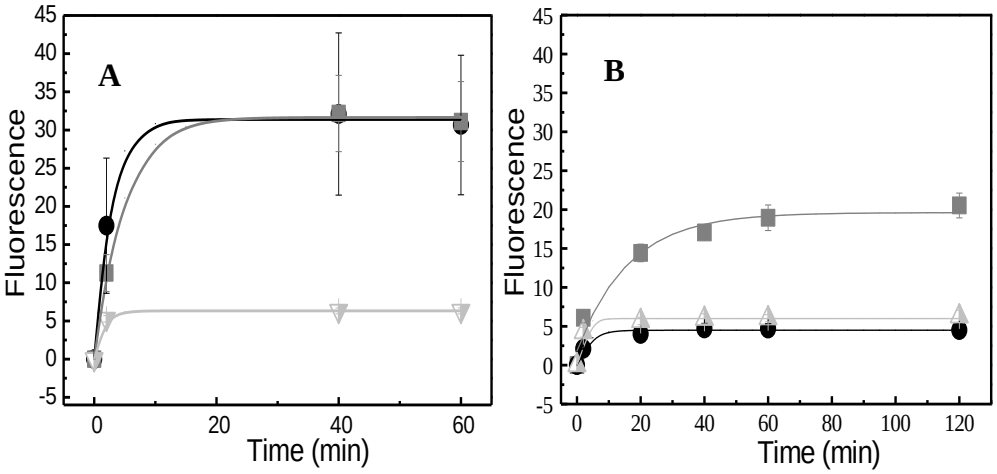

Figure 3.22. Kinetic analysis of Amplex Red reaction with Wt-CYP119 (●), N-His-CYP119 (■) and C-His-CYP119 (△) at room temperature (A) and 65°C (B). Reactions were performed using 10 μM Amplex Red, 1.5 mM H_2O_2 and 1.5 μM enzyme in 50 mM sodium phosphate buffer at pH 7.4. The average of the emission values of the resorufin at 580 nm from three independent measurements were used. The data are fit to one phase association kinetics.

The further investigation of catalytic activity of N-His-CYP119 was followed by UV-Visible spectra. The Figure 3.23A has shown the product formation (resorufin) with the increasing time. The first spectrum was taken as soon as the reaction had started, and the spectrum taken up to 3 hours (taken at 0, 2, 5, 10, 20, 30, 45, 60, 90, 120, 150, 180, and 270 minutes). The CYP119 Soret and the resorufin give a peak at 415 nm and 571 nm at UV-Vis Spectroscopy, respectively. The time course of changes in absorbance at 570 nm and 415 nm (CYP119 Soret) in the same reaction is shown Figure 3.23C.

Since the highest activity and stability were observed for N-His-CYP119, the kinetic parameters for Amplex Red oxidation catalyzed by this protein were investigated. Previous studies have shown that CYP119 can catalyze Amplex Red oxidation,[25] however, kinetic parameters and the yield of this reaction have not been investigated. Using the extinction coefficient of resorufin at 570 nm,[38] only 16% product formation was observed in the presence of 10 μM Amplex Red, 1.5 mM H_2O_2 and 1.5 μM

N-His-CYP119 after 3 hours (Figure 3.23); this corresponds to a single turnover of the enzyme. Therefore, the yield of Amplex Red oxidation is very low. Indeed, when Amplex Red oxidation was monitored in the presence of increasing concentration of H_2O_2, the k_{cat} obtained was only $7.5 \pm 3.2 \times 10^{-4}$ s^{-1}. In comparison, previous studies have determined the k_{cat} for oxidation of styrene for CYP119[25] as 1.3 s^{-1}. Therefore, Amplex Red appears to be a worse substrate for CYP119 compared to styrene.

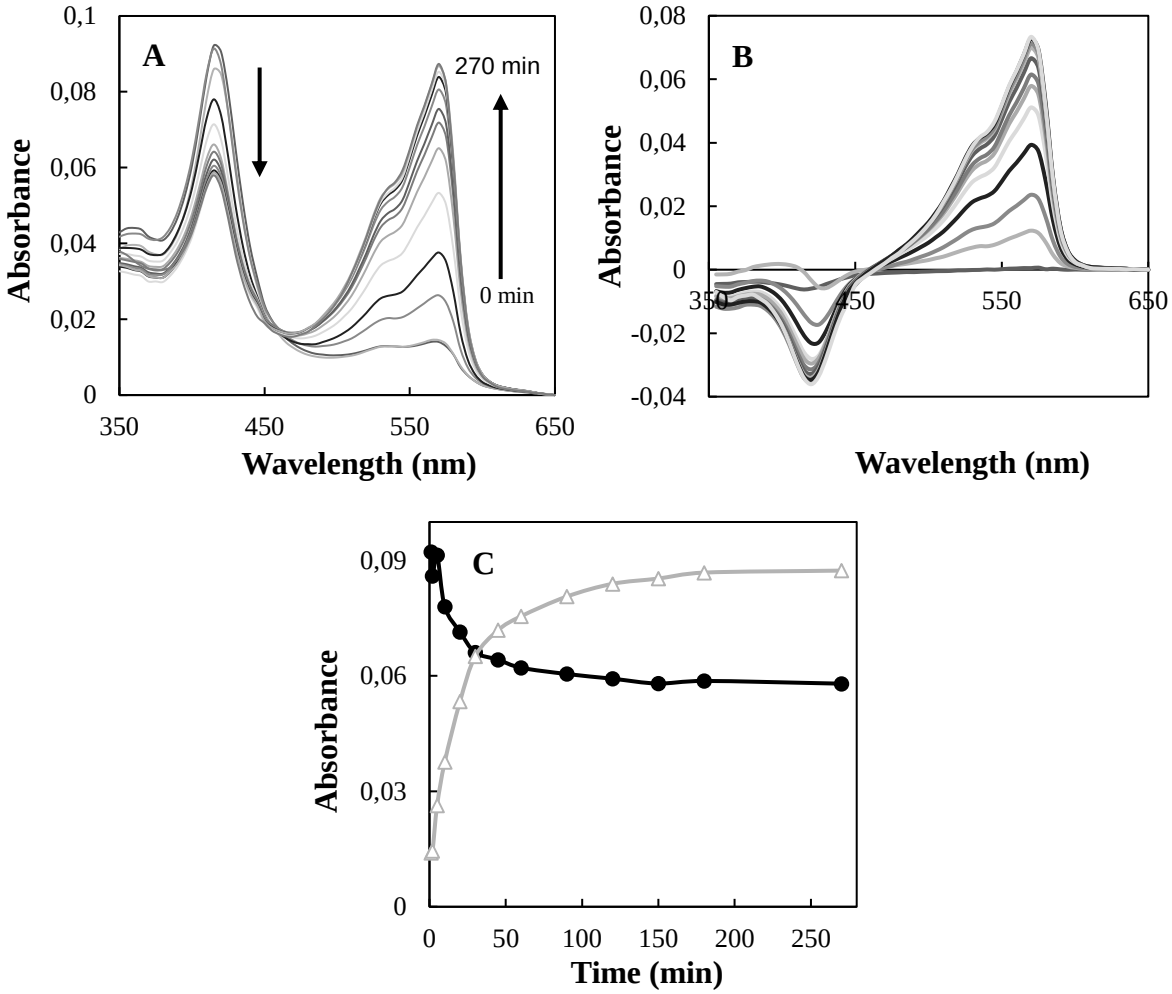

Figure 3.23. Changes in the UV-Visible spectra during Amplex Red oxidation by H_2O_2 in the presence of N-His-CYP119. A, the UV-Visible spectra taken at 0, 2, 5, 10, 20, 30, 45, 60, 90, 120, 150, 180 and 270 minutes after addition of H_2O_2. B, the UV-Visible difference spectra. The reaction components were 10 μM Amplex Red, 1.5 mM H_2O_2 and 1.5 μM N-His-CYP119 in 50 mM sodium phosphate buffer at pH 7.4. C, time course of changes in absorbance at 570 nm (△, resorufin) and 415 nm (●, CYP119 Soret) in the same reaction.

To determine the kinetic parameters for Amplex Red oxidation by N-His-CYP119, formation of resorufin was followed by absorbance at 570 nm during the reaction of Amplex Red (10 μM) with H_2O_2 (0.25 - 2 mM) in the presence of N-His-CYP119 (1.5 μM). As seen in Figure 3.23C, the formation of resorufin increases linearly with time during the first 30 minutes of the reaction therefore, resorufin concentration at 30 min was used in determination of kinetic parameters. The dependence of initial rate on H_2O_2 concentration is shown in Figure 3.24. Using data at Figure 3.23, the K_M was determined to be 1.4 ± 1.1 mM and k_{cat} was 7.5 ± 3.2 × 10^{-4} s^{-1} for N-His-CYP119 (in the presence of 10 μM Amplex Red).

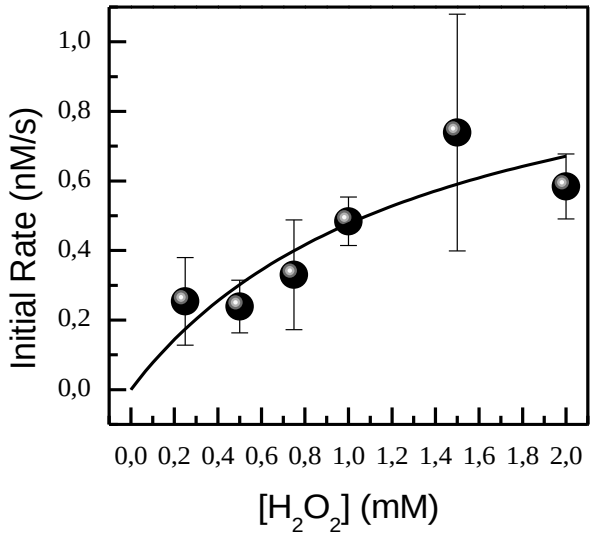

Figure 3.24. Determination of the kinetic parameters of Amplex Red oxidation by H_2O_2 in the presence of N-His-CYP119. Reactions contained 10 μM Amplex Red, 1.5 μM N-His-CYP119 and 0.2 - 2 mM of H_2O_2 in 50 mM sodium phosphate buffer, pH 7.4.

The activity test with N-His-CYP119 at 90 °C was showed that it has similar activity to compared to activity non-incubated N-His-CYP119 (Figure 3.25). The product formation was the same first 18 minutes at both temperatures. After 50 minutes of the reaction product formation decreased 1.45-fold at 90 °C as seen in Figure 3.25.

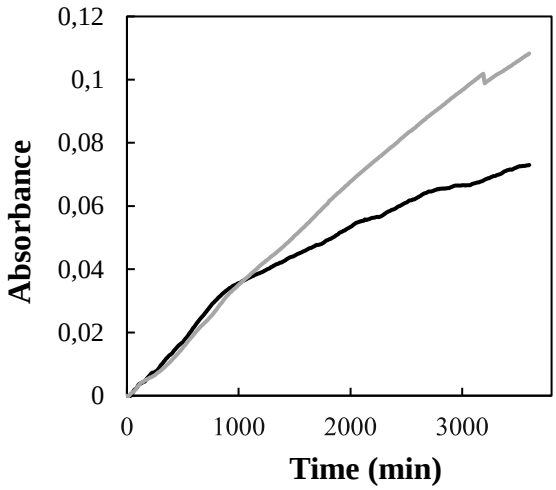

Figure 3.25. Determination of Amplex Red oxidation by H_2O_2 in the presence of N-His-CYP119 at room temperature (grey) and 90 °C (black). Reactions contained 10 µM Amplex Red, 1.5 µM N-His-CYP119 and 1 mM of H_2O_2 in 50 mM sodium phosphate buffer, pH 7.4.

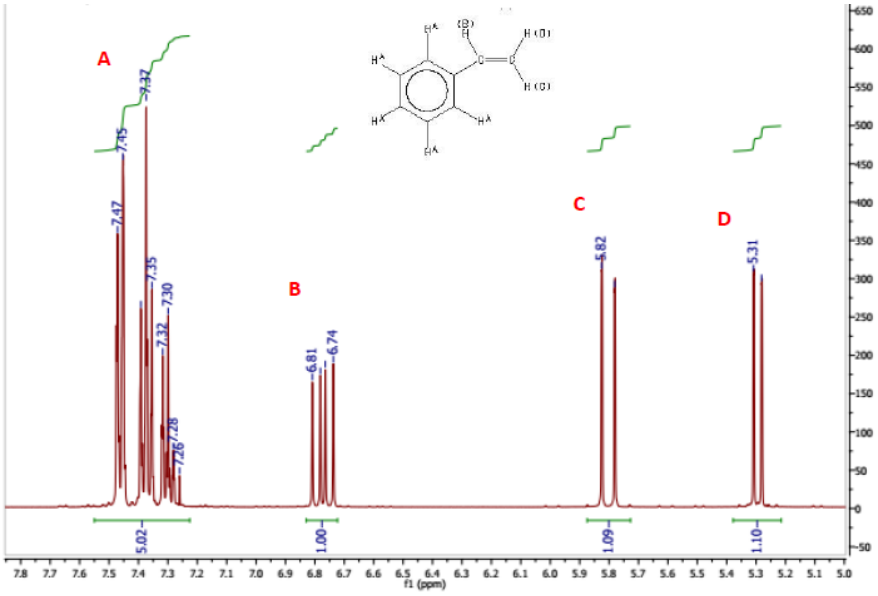

Figure 3.26. The ^{1}H-NMR spectrum of styrene in chloroform

3.5.4. HPLC Analysis of Styrene Epoxidation with N-His-CYP119

The structure of styrene in chloroform was verified by ^{1}H-NMR (Figure 3.26). The epoxidation of 1 mM styrene was catalyzed with 12.5 µM N-His-CYP119 in the

presence of 5 mM tertbutyl hydroperoxide (TBHP) at room temperature and 65 °C. The product (styrene oxide) was monitored by HPLC analysis. The retention time styrene (2.02 min.) and styrene oxide (1.46) are shown Figure 3.27. The previous studies has shown that the retention time of styrene oxide is about 1.8 minutes[36]. Here, second oxidation of styrene may be occurred. The styrene may be oxidized to another molecule instead of styrene.

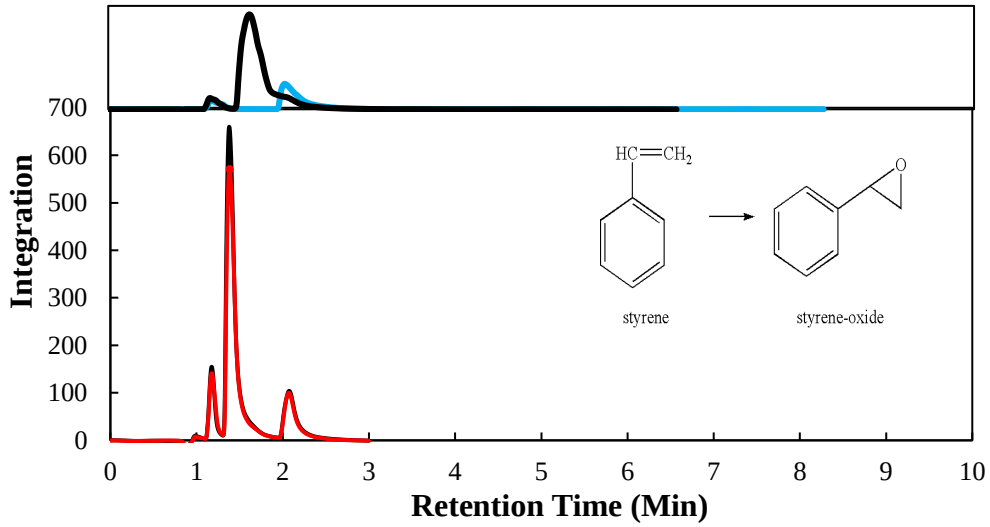

Figure 3.27. HPLC analysis of styrene (1mM) epoxidation reaction with N-His-CYP119 (12.5 μM) in the presence of TBHP (5 mM) in 50 mM glycine buffer (pH: 8.5). 2.08 min styrene; 1.38 min shows the product (styrene epoxide) resulting from the reaction and 1.18 min shows the peak from the glycine buffer. The reactions are incubated at room temperature (black) and 65 °C (dash) for 10 minutes. Inset: The Styrene (2.07; grey) and Styrene oxide (1,68; black) retention times.

CHAPTER 4

CONCLUSION

The development of molecular biology and genetic techniques in protein and enzyme engineering have increased the application of biocatalysis in the chemical and pharmaceutical industry. In particular, the industrial use of thermophilic enzymes, which are resistant to high temperatures, have increased. In this study, optimization of expression and isolation of the thermophilic CYP119 was performed. Histidine tags, which are frequently used in protein studies, has provided an easy protein purification and high yields in short time. Here, His-tags were cloned to N- and C-terminal of the CYP119s. After the expression of His-tagged CYP119 under optimum conditions, N-His-CYP119 and C-His-CYP119 were isolated and purified up to 95% by IMAC. Then, the spectroscopic features of CYP119 with His-tags were analysed and compared to Wt-CYP119. The results showed that cloned histidine tags can change the spectroscopic features of CYP119. From the thermostability analyses the C-His-CYP119 is more stable than the N-His-CYP119 even at 90 °C.

Amplex Red oxidation of C-His-CYP119, N-His-CYP119 and Wt-CYP119 were investigated using H_2O_2 as an oxidant. The results showed that the N-His-CYP119 was the more active than C-His-CYP119 and had a similar activity of Wt-CYP119 at room temperature. However, the activities of all the enzymes showed a small decrease at 65 °C, the N-His-CYP119 is more active than the C-His-CYP119 and Wt-CYP119 at 65 °C. In addition, styrene epoxidation was catalysed by the N-His-CYP119 in the presence of TBHP. Styrene epoxide formation was monitored by HPLC after 10 minutes of reaction. All results have demonstrated the histidine tags cloned into the protein changed protein stability and activity.

In this thesis, for the first time the optimal conditions have been identified to express and isolate of the thermostable CYP119. The spectroscopic characterization and activity of Wt-CYP119 and his-tagged variants have been investigated. The Amplex Red oxidation with N-His-CYP119 was monitored in the presence of increasing concentrations of H_2O_2. For the first time, kinetic parameters of CYP119 for the Amplex

Red oxidation with H_2O_2 have been determined. In addition, first time importance of histidine tags on the stability and activity of his-tagged CYP119s has been compared with Wild type CYP119. N-His-CYP119 showed higher stability and activity compared to C-His-CYP119; therefore, it is a good candidate for possible industrial applications. The His-tag in N-His-CYP119 is connected to the protein through a thrombin cleavage site, therefore, this construct can be used to obtain tag-free Wt-CYP119 with additional purification steps. These results showed that His-tags can influence CYP119 mechanisms and one should be careful using His-tags especially in mechanistic studies.

REFERENCES

1. Schulz, S.; Girhard, M.; Urlacher, V. B., Biocatalysis: Key to Selective Oxidations. *ChemCatChem* **2012**, *4* (12), 1889-1895.

2. Bornscheuer, U. T.; Huisman, G. W.; Kazlauskas, R. J.; Lutz, S.; Moore, J. C.; Robins, K., Engineering the third wave of biocatalysis. *Nature* **2012**, *485* (7397), 185-194.

3. McLean, M. A.; Maves, S. A.; Weiss, K. E.; Krepich, S.; Sligar, S. G., Characterization of a Cytochrome P450 from the Acidothermophilic Archaea *Sulfolobus solfataricus.* **1998**.

4. Schmidt-Dannert, C.; Lopez-Gallego, F., A roadmap for biocatalysis - functional and spatial orchestration of enzyme cascades. *Microb Biotechnol* **2016,** *9* (5), 601-9.

5. Yano, J. K.; Koo, L. S.; Schuller, D. J.; Li, H.; Ortiz de Montellano, P. R.; Poulos, T. L., Crystal structure of a thermophilic cytochrome P450 from the archaeon Sulfolobus solfataricus. *J Biol Chem* **2000**, *275* (40), 31086-92.

6. Jung, S. T.; Lauchli, R.; Arnold, F. H., Cytochrome P450: taming a wild type enzyme. *Curr Opin Biotechnol* **2011**, *22* (6), 809-17.

7. Cook, D. J.; Finnigan, J. D.; Cook, K.; Black, G. W.; Charnock, S. J., Cytochromes P450: History, Classes, Catalytic Mechanism, and Industrial Application. *Adv Protein Chem Struct Biol* **2016**, *105*, 105-26.

8. Denisov , I. G.; Hung , S. C.; Weiss , K. E.; McLean , M. A.; Shiro , Y.; Parkb, S. Y.; Championc, P. M.; Sligar, S. G., Characterization of the oxygenated intermediate of the thermophilic cytochrome P450 CYP119. **2001**.

9. Guengeric, F. P., Reactions and Significance of Cytochrome P-450 Enzymes. *The Journal of Biological Chemistry* **1991**, *266*;16 (June 5), 10019-10022.

10. Guengerich, F. P.; Munro, A. W., Unusual cytochrome p450 enzymes and reactions. *J Biol Chem* **2013**, *288* (24), 17065-73.

11. Porter, P. D.; Coon, M. J., cytochrome p-450 multiplicity of isoforms, substrates, and catalytic and regulatory mechanisms. *The journal of biological chemistry* **1991**, *Vol. 266*, No. 21 (Issue of July 25), 13469-13472.

12. Roduner, E.; Kaim, W.; Sarkar, B.; Urlacher, V. B.; Pleiss, J.; Gläser, R.; Einicke, W.-D.; Sprenger, G. A.; Beifuß, U.; Klemm, E.; Liebner, C.; Hieronymus, H.; Hsu, S.-F.; Plietker,

B.; Laschat, S., Selective Catalytic Oxidation of C□H Bonds with Molecular Oxygen. *ChemCatChem* **2013**, *5* (1), 82-112.

13. Klingenberg, M., Pigments of rat liver microsomes. Archives of Biochemistry and *Biophysics* **2003**, *409*, 2-6.

14. Nelson, D. R., The Cytochrome P450 Homepage. **2009**.

15. Nelson, D. R., A world of cytochrome P450s. *Philos Trans R Soc Lond B Biol Sci* **2013**, *368* (1612), 20120430.

16. Nelson, D. R., Cytochrome P450 diversity in the tree of life. *Biochim Biophys Acta* **2017**, *1866* (1), 141-154.

17. C, A., Hasemann.; R, G., Kurumbail.; S, S., Boddupalli.; J, A., Peterson.; J, D., Structure and function of cytochromes P450: a comparative analysis of three crystal structures. *Current Biology* **1995**, *2* (1), 41-62.

18. Yasuda, K.; Sugimoto, H.; Hayashi, K.; Takita, T.; Yasukawa, K.; Ohta, M.; Kamakura, M.; Ikushiro, S.; Shiro, Y.; Sakaki, T., Protein engineering of CYP105s for their industrial uses. *Biochim Biophys Acta 2018,* **1866** (1), 23-31.

19. Wright, R. L.; Harris, K.; Solow, B.; White, R. H.; Kennelly, P. J., Cloning of a potential cytochrome P450 from the Archaeon. **1996**.

20. BRocK, T. D.; BRocK, K. M.; BELLY, R. T.; WEIss, R., L., Sulfolobus: A New Genus of Sulfur-Oxidizing Bacteria Living at Low pH and High Temperature. *Arch. Mikrobiol* **1972**, *84*, 54-68.

21. Park, S. Y.; Yamane, K.; Adachi, S.; Shiro, Y.; Weissb, K. E.; Sligar, S. G., Crystallization and preliminary X-ray diffraction analysis of a cytochrome P450 (CYP119) from *Sulfolobus solfataricus*. *Biological Crystallography* **2000**, *D56*, 1173-1175.

22. Groves, J. T., *Cytochrome P450 Structure, Mechanism, and Biochemistry*. Montellano, P. R. O. d., Ed. 2004.

23. *Sulfolobus acidocaldarius*. https://microbewiki.kenyon.edu/index.php/*Sulfolobus_acidocaldarius* (accessed December 23, 2018

24. Bears And Bison And... Thermoacidophiles. https://www.theodysseyonline.com/bear-and-bison-and-thermoacidophiles (accessed October 30, 2017).

25. Rabe, K. S.; Kiko, K.; Niemeyer, C. M., Characterization of the peroxidase activity of CYP119, a thermostable P450 from Sulfolobus acidocaldarius. *Chembiochem* **2008**, *9* (3), 420-5.

26. Basudhar, D.; Madrona, Y.; Kandel, S.; Lampe, J. N.; Nishida, C. R.; de Montellano, P. R., Analysis of cytochrome P450 CYP119 ligand-dependent conformational dynamics by two-dimensional NMR and X-ray crystallography. *J Biol Chem* **2015**, *290* (16), 10000-17.

27. Wachowska, M.; Muchowicz, A.; Firczuk, M.; Gabrysiak, M.; Winiarska, M.; Wańczyk, M.; Bojarczuk, K.; Golab, J., Aminolevulinic Acid (ALA) as a Prodrug in Photodynamic Therapy of Cancer. *Molecules* **2011**, (16), 4140-4164.

28. Bornhorst, J. A.; Falke, J. J., Purification of Proteins Using Polyhistidine Affinity Tags. *Methods Enzymol* **2010**, *326*, 245–254.

29. Graslund, S.; Nordlund, P.; Weigelt, J.; Hallberg, B. M.; Bray, J.; Gileadi, O.; Knapp, S.; Oppermann, U.; Arrowsmith, C.; Hui, R.; Ming, J.; dhe-Paganon, S.; Park, H. W.; Savchenko, A.; Yee, A.; Edwards, A.; Vincentelli, R.; Cambillau, C.; Kim, R.; Kim, S. H.; Rao, Z.; Shi, Y.; Terwilliger, T. C.; Kim, C. Y.; Hung, L. W.; Waldo, G. S.; Peleg, Y.; Albeck, S.; Unger, T.; Dym, O.; Prilusky, J.; Sussman, J. L.; Stevens, R. C.; Lesley, S. A.; Wilson, I. A.; Joachimiak, A.; Collart, F.; Dementieva, I.; Donnelly, M. I.; Eschenfeldt, W. H.; Kim, Y.; Stols, L.; Wu, R.; Zhou, M.; Burley, S. K.; Emtage, J. S.; Sauder, J. M.; Thompson, D.; Bain, K.; Luz, J.; Gheyi, T.; Zhang, F.; Atwell, S.; Almo, S. C.; Bonanno, J. B.; Fiser, A.; Swaminathan, S.; Studier, F. W.; Chance, M. R.; Sali, A.; Acton, T. B.; Xiao, R.; Zhao, L.; Ma, L. C.; Hunt, J. F.; Tong, L.; Cunningham, K.; Inouye, M.; Anderson, S.; Janjua, H.; Shastry, R.; Ho, C. K.; Wang, D.; Wang, H.; Jiang, M.; Montelione, G. T.; Stuart, D. I.; Owens, R. J.; Daenke, S.; Schutz, A.; Heinemann, U.; Yokoyama, S.; Bussow, K.; Gunsalus, K. C., Protein production and purification. *Nat Methods* **2008**, *5* (2), 135-46.

30. Booth, W. T.; Schlachter, C. R.; Pote, S.; Ussin, N.; Mank, N. J.; Klapper, V.; Offermann, L. R.; Tang, C.; Hurlburt, B. K.; Chruszcz, M., Impact of an N-terminal Polyhistidine Tag on Protein Thermal Stability. *ACS Omega* **2018**, *3* (1), 760-768.

31. Panek, A.; Pietrow, O.; Filipkowski, P.; Synowiecki, J., Effects of the polyhistidine tag on kinetics and other properties of trehalose synthase from Deinococcus geothermalis. *Acta Biochimica Polonica* **2013**, *60* (2), 163-166.

32. Sabaty, M.; Grosse, S.; Adryanczyk, G.; Boiry, S.; Biaso, F.; Arnoux, P.; Pignol, D., Detrimental effect of the 6 His C-terminal tag on YedY enzymatic activity and influence of the TAT signal sequence on YedY synthesis. *BMC Biochemistry* **2013**, 14-28.

33. Majorek, K. A.; Kuhn, M. L.; Chruszcz, M.; Anderson, W. F.; Minor, W., Double trouble-Buffer selection and His-tag presence may be responsible for nonreproducibility of biomedical experiments. *Protein Sci* **2014**, *23* (10), 1359-68.

34. Koo, L. S.; Tschirret-Guth, R. A.; Straub, W. E.; Loccoz, P. M.; Loehr§, T. M.; Montellano, P. R. O., The Active Site of the Thermophilic CYP119 from Sulfolobus solfataricus. *The Journal of Biological Chemistry* **2000**, *275* (19), 14112–14123.

35. Suzuki, R.; Hirakawa, H.; Nagamune, T., Electron donation to an archaeal cytochrome P450 is enhanced by PCNA-mediated selective complex formation with foreign redox proteins. *Biotechnol J* **2014**, *9* (12), 1573-81.

36. Zhang, C.; Li, J.; Yang, B.; He, F.; Yang, S.-Y.; Yu, X.-Q.; Wang, Q., Enhanced turnover rate and enantioselectivity in the asymmetric epoxidation of styrene by new T213G mutants of CYP 119. *RSC Adv.* **2014**, *4* (52), 27526-27531.

37. Towne, V.; Will, M.; Oswald, B.; Zhao, Q., Complexities in horseradish peroxidase-catalyzed oxidation of dihydroxyphenoxazine derivatives: appropriate ranges for pH values and hydrogen peroxide concentrations in quantitative analysis. *Anal Biochem* **2004**, *334* (2), 290-6.

38. Zhou, M.; Diwu, Z.; Panchuk-Voloshina, N.; Haugland, R. P., A Stable Nonfluorescent Derivative of Resorufin for the Fluorometric Determination of Trace Hydrogen Peroxide: Applications in Detecting the Activity of Phagocyte NADPH Oxidase and Other Oxidases. *Analitical Biochemistry* **1997**, *253*, 162–168.

APPENDIX A

VECTOR MAPS

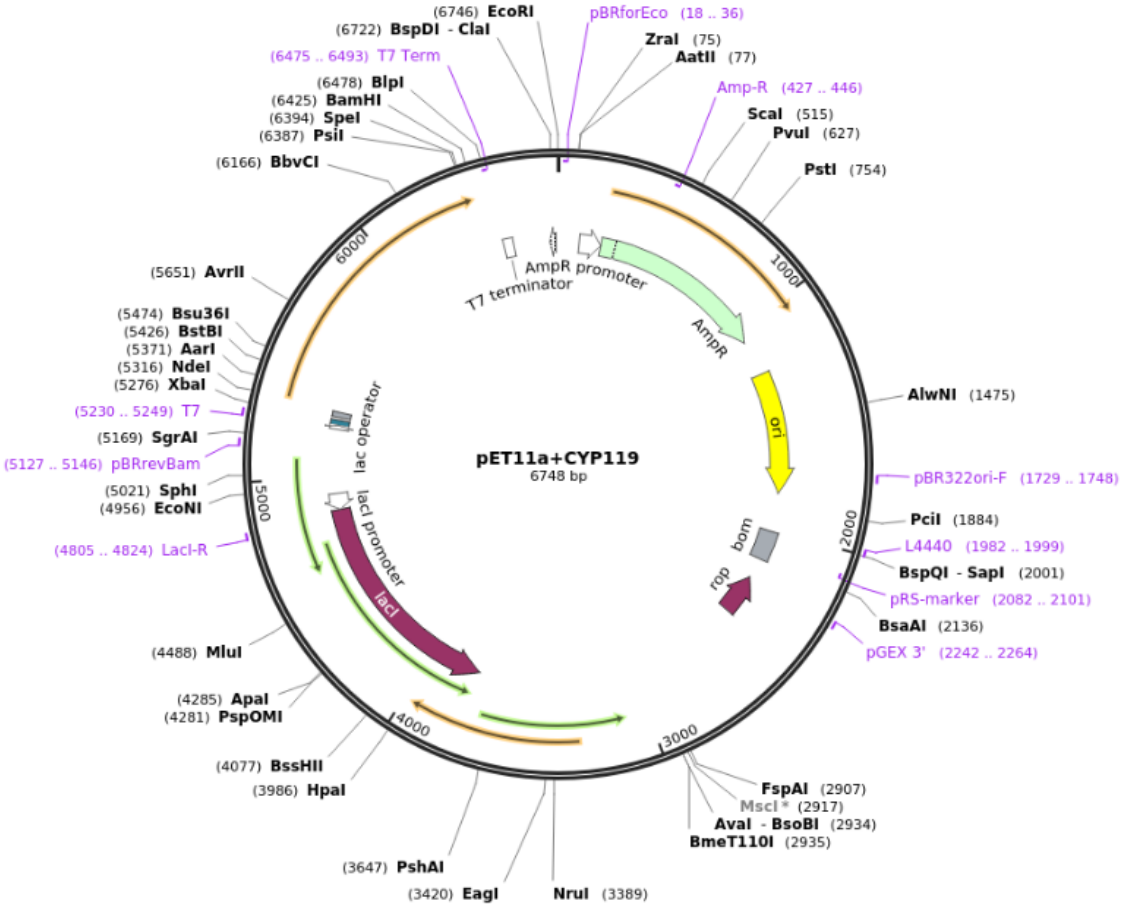

Figure A.1. pET11a+CYP119 vector map. The illustration was created in SnapGene Viewer

pET-14b sequence landmarks	
T7 promoter	646-662
T7 transcription start	645
His•Tag coding sequence	554-571
Multiple cloning sites	
(*Nde* I -*Bam*H I)	510-526
T7 terminator	404-450
pBR322 origin	2845
bla coding sequence	3606-4463

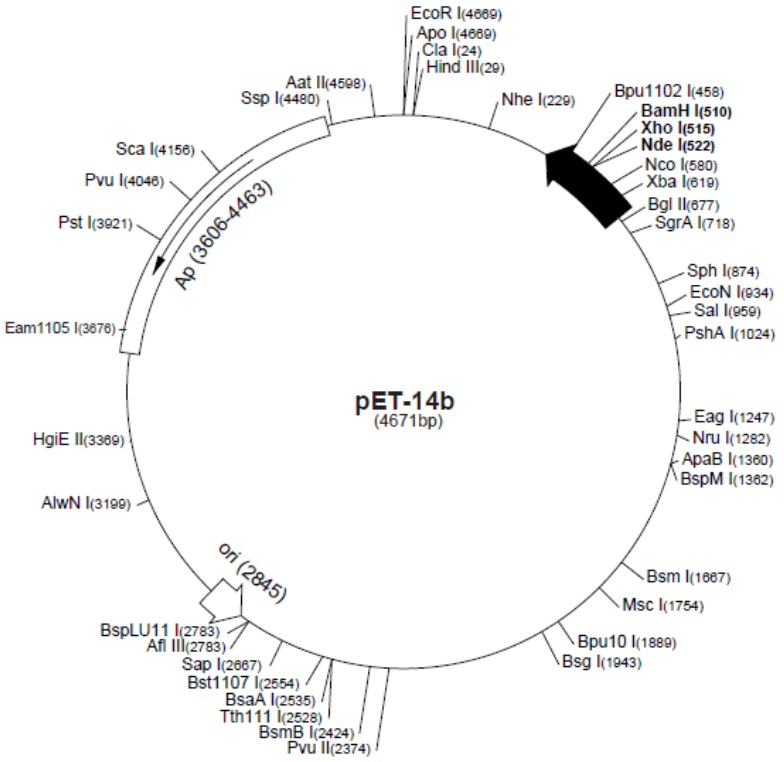

Figure A.2. pET-14b vector map

pET-20b(+) sequence landmarks	
T7 promoter	353-369
T7 transcription start	352
pelB coding sequence	224-289
Multiple cloning sites	
(*Nco* I - *Xho* I)	158-225
His•Tag coding sequence	140-157
T7 terminator	26-72
pBR322 origin	1500
bla coding sequence	2261-3118
f1 origin	3250-3705

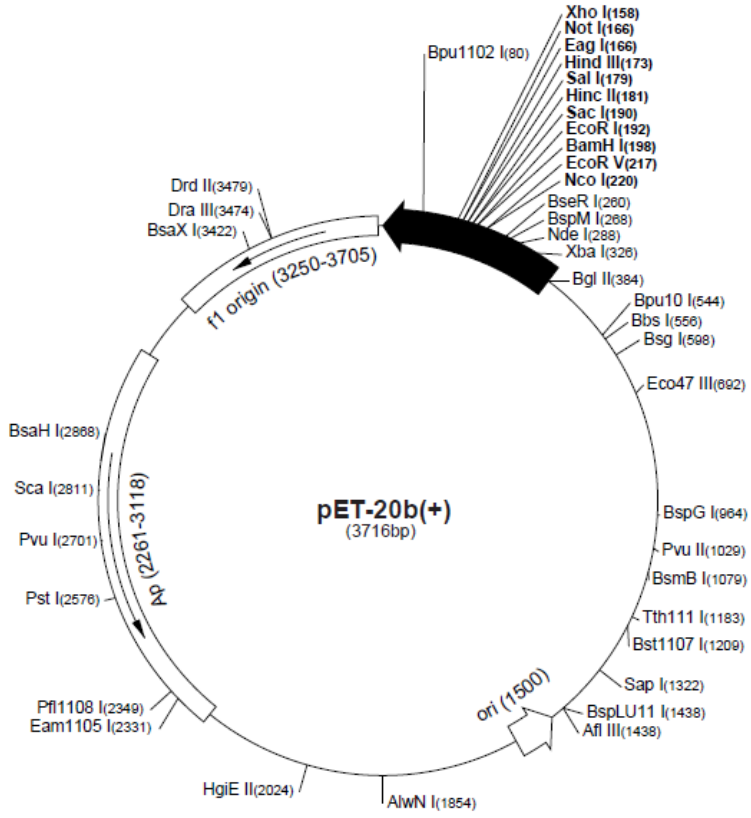

Figure A.3. pET-20b (+) vector map

APPENDIX B

PROTEIN SEQUENCES

Wild type CYP119

MYDWFSEMRKKDPVYYDGNIWQVFSYRYTKEVLNNFSKFSSDLTGYHERLED
LRNGKIRFDIPTRYTMLTSDPPLHDELRSMSADIFSPQKLQTLETFIRETTRSLLDS
IDPREDDIVKKLAVPLPIIVISKILGLPIEDKEKFKEWSDLVAFRLGKPGEIFELGK
KYLELIGYVKDHLNSGTEVVSRVVNSNLSDIEKLGYIILLLIAGNETTTNLISNSV
IDFTRFNLWQRIREENLYLKAIEEALRYSPPVMRTVRKTKERVKLGDQTIEEGEY
VRVWIASANRDEEVFHDGEKFIPDRNPNPHLSFGSGIHLCLGAPLARLEARIAI
EFSKRFRHIEILDTEKVPNEVLNGYKRLVVRLKSNE*

CYP119 with N-terminal His-Tag (N-His-CYP119). The bold aminoacids are showed added aminoacids and the histidine residues. The thrombin cleavage site is underlined

MGSSHHHHHHSSG<u>LVPRGS</u>HMYDWFSEMRKKDPVYYDGNIWQVFSYRYTK
EVLNNFSKFSSDLTGYHERLEDLRNGKIRFDIPTRYTMLTSDPPLHDELRSMSAD
IFSPQKLQTLETFIRETTRSLLDSIDPREDDIVKKLAVPLPIIVISKILGLPIEDKEKF
KEWSDLVAFRLGKPGEIFELGKKYLELIGYVKDHLNSGTEVVSRVVNSNLSDIE
KLGYIILLLIAGNETTTNLISNSVIDFTRFNLWQRIREENLYLKAIEEALRYSPPVM
RTVRKTKERVKLGDQTIEEGEYVRVWIASANRDEEVFHD GEKFIPDRN
PNPHLSFGSGIHLCLGAPLARLEARIAIEEFSKRFRHIEILDTEKVPNEVL
NGYKRLVVRLKSNE*

CYP119 with C-terminal His-Tag (C-His-CYP119). The bold aminoacids are showed added aminoacids and the histidine residues

MYDWFSEMRKKDPVYYDGNIWQVFSYRYTKEVLNNFSKFSSDLTGYHERLED
LRNGKIRFDIPTRYTMLTSDPPLHDELRSMSADIFSPQKLQTLETFIRETTRSLLDS
IDPREDDIVKKLAVPLPIIVISKILGLPIEDKEKFKEWSDLVAFRLGKPGEIFELGK
KYLELIGYVKDHLNSGTEVVSRVVNSNLSDIEKLGYIILLLIAGNETTTNLISNSV
IDFTRFNLWQRIREENLYLKAIEEALRYSPPVMRTVRKTKERVKLGDQTIEEGEY
VRVWIASANRDEEVFHDGEKFIPDRNPNPHLSFGSGIHLCLGAPLARLEARIAIE
EFSKRFRHIEILDTEKVPNEVLNGYKRLVVRLKSNE **SVDKLAAALEHHHHHH***